NASA Technical Memorandum 4448

An Improved CAMRAD Model for Aeroelastic Stability Analysis of the XV-15 With Advanced Technology Blades

C. W. Acree, Jr.
Ames Research Center
Moffett Field, California

National Aeronautics and Space Administration

Office of Management

Scientific and Technical Information Program

1993

REPORT DOCUMENTATION PAGE

Form Approved
OMB No. 0704-0188

1. AGENCY USE ONLY *(Leave blank)*	2. REPORT DATE	3. REPORT TYPE AND DATES COVERED
	March 1993	Technical Memorandum

4. TITLE AND SUBTITLE
An Improved CAMRAD Model for Aeroelastic Stability Analysis of the XV-15 With Advanced Technology Blades

5. FUNDING NUMBERS
WU 505-59-36

6. AUTHOR(S)
C. W. Acree, Jr.

7. PERFORMING ORGANIZATION NAME(S) AND ADDRESS(ES)
Ames Research Center
Moffett Field, CA 94035-1000

8. PERFORMING ORGANIZATION REPORT NUMBER
A-92022

9. SPONSORING/MONITORING AGENCY NAME(S) AND ADDRESS(ES)
National Aeronautics and Space Administration
Washington, DC 20546-0001

10. SPONSORING/MONITORING AGENCY REPORT NUMBER
NASA TM-4448

11. SUPPLEMENTARY NOTES
Point of Contact: C. W. Acree, Ames Research Center, MS 237-5, Moffett Field, CA 94035-1000
(415) 604-5423

12a. DISTRIBUTION/AVAILABILITY STATEMENT
Unclassified — Unlimited
Subject Category 05

12b. DISTRIBUTION CODE

13. ABSTRACT *(Maximum 200 words)*

In pursuit of higher performance, the XV-15 Tiltrotor Research Aircraft was modified by the installation of new composite rotor blades. Initial flights with the Advanced Technology Blades (ATBs) revealed excessive rotor control loads that were traced to a dynamic mismatch between the blades and the aircraft control system. The analytical models of both the blades and the mechanical controls were extensively revised for use by the CAMRAD computer program to better predict aeroelastic stability and loads. This report documents the most important revisions and discusses their effects on aeroelastic stability predictions for airplane-mode flight. The ATBs may be flown in several different configurations for research, including changes in blade sweep and tip twist. The effects on stability of 1° and 0° sweep are illustrated, as are those of twisted and zero-twist tips. This report also discusses the effects of stiffening the rotor control system, which was done by locking out lateral cyclic swashplate motion with shims.

14. SUBJECT TERMS	15. NUMBER OF PAGES
CAMRAD Advanced techno.ogy, Blades, XV-15, Aeroelastic stability	60
	16. PRICE CODE: A04

17. SECURITY CLASSIFICATION OF REPORT	18. SECURITY CLASSIFICATION OF THIS PAGE	19. SECURITY CLASSIFICATION OF ABSTRACT	20. LIMITATION OF ABSTRACT
Unclassified	Unclassified		

SYMBOLS

General

C_t/σ	thrust coefficient, divided by solidity
K	control-system stiffness matrix (inverted form)
q_{f_n}	nth fuselage dynamic mode (n = 1 to 4 are symmetric, n = 5 to 8 are antisymmetric)
R	rotor radius

Control System

M_0	collective pitch moment, ft·lb
M_{1C}	lateral cyclic moment, ft·lb
M_{1S}	longitudinal cyclic moment, ft·lb
θ_0	collective pitch measured at the blade root, rad
θ_{1C}	lateral cyclic pitch, rad
θ_{1S}	longitudinal cyclic pitch, rad
θ_{75}	collective pitch measured at 75% R, rad

Aeroelastic Modes

$X+1$	advancing or progressive mode, for any mode X
$X-1$	retreating or regressive mode
β_G	rotor-gimbal mode
β_n	nth blade-bending mode (flap and/or lead-lag)
θ_n	nth blade-torsion mode
λ_u	rotor inflow
Ψ_E	engine-speed mode
Ψ_I	interconnect-shaft-speed mode (antisymmetric)
Ψ_S	rotor-speed mode (symmetric)

Note: The above notation generally follows that of reference 5. The first collective bending and torsion modes are labeled β_0 and θ_0, respectively, but the first progressive and regressive modes are labeled β_1+1, θ_1+1, β_1-1, and θ_1-1.

SUMMARY

In pursuit of higher performance, the XV-15 Tiltrotor Research Aircraft was modified by the installation of new composite rotor blades. Initial flights with the Advanced Technology Blades (ATBs) revealed excessive rotor control loads that were traced to a dynamic mismatch between the blades and the aircraft control system. The analytical models of both the blades and the mechanical controls were extensively revised for use by the CAMRAD computer program to better predict aeroelastic stability and loads. This report documents the most important revisions and discusses their effects on aeroelastic stability predictions for airplane-mode flight. The ATBs may be flown in several different configurations for research, including changes in blade sweep and tip twist. The effects on stability of 1° and 0° sweep are illustrated, as are those of twisted and zero-twist tips. This report also discusses the effects of stiffening the rotor control system, which was done by locking out lateral cyclic swashplate motion with shims.

INTRODUCTION

The XV-15 Tiltrotor Research Aircraft (fig. 1), developed by Bell Helicopters Textron under NASA/Army contract, has been flying for several years. To save development time and cost, the initial configuration utilized much existing hardware; one deliberate compromise was the use of metal rotor blades that were sized for a lighter airframe and less powerful engines. In 1982, a project was initiated to develop new rotor blades to allow the XV-15 to more closely achieve its full performance potential. The resulting Advanced Technology Blades (ATBs) were built by the Boeing Helicopter Company under contract to NASA.

The ATBs (fig. 2) are constructed almost entirely of composite materials, the exceptions being the pitch-bearing housing and such items as fasteners and balance weights. Major design features, relative to the metal blades, are higher solidity, a compound tapered planform (fig. 3), greater twist, replaceable cuffs and tips, and adjustable sweep. The ATB development prior to flight test is described in reference 1, details of the structural design are given in reference 2, and the aerodynamic design is discussed in reference 3. Additional design data are given in appendix A.

Initial flight tests in 1988 revealed extremely high control-system loads at 3/rev that severely restricted the flight envelope. The problem had not been seen during earlier whirl-stand tests (ref. 4). It was subsequently discovered that the analytical model used to predict performance, loads, and aeroelastic stability contained several crucial errors. The original model was developed by Boeing for use with the CAMRAD computer program (ref. 5). The most important errors were underestimation of blade-pitch inertia and inadequate modeling of XV-15 control-system flexibility. A ground test was undertaken by NASA to determine the sources and magnitude of control flexibility. The XV-15/ATB model was extensively revised with a more accurate representation of the blade properties, and CAMRAD was modified to better model the effects of control-system flexibility. Significant changes were also made to the drive-train model.

A close examination of the analysis revealed that CAMRAD does not properly compute all drive-train dynamics, even when given correct input data. The engine shaft (power turbine) is modeled as only a quasi-static degree of freedom for antisymmetric modes. This degree of freedom is critical for aeroelastic analysis of the ATBs, because the drive train strongly couples with collective blade modes. CAMRAD still reveals the effects of parametric changes in the model, but the predicted frequencies of antisymmetric modes are unreliable. Therefore, for coalescence-sensitive phenomena such as pitch-flap instability, the antisymmetric results are in error. Fortunately for the XV-15/ATB study, the error drives important modes toward coalescence, thereby underpredicting stability margins. Symmetric modes are unaffected.

With the new XV-15/ATB model, CAMRAD correctly predicted the high loads seen in flight. Those predictions are reported in reference 6, along with key flight data. Reduced aeroelastic stability margins were also predicted for the ATBs; an example based on the original model is given in figure 4, which is an eigenvalue plot in root-locus format illustrating the effects of control-system flexibility on stability[1] in airplane mode. The blades were not adequately counterbalanced in pitch to preclude the pitch-flap instability seen at 60% control stiffness at only 250 KTAS (the collective torsion mode, θ_0). At 80% stiffness, a second antisymmetric mode (collective torsion coupled with first bending and the drive train, $\theta_0/\beta_0/\Psi_1$) is almost neutrally stable,

[1]The notation in the stability plots generally follows that of reference 5. For example, β_2/Ψ_E is the second-bending mode coupled with the (symmetric) engine-shaft mode. Because of the frequent, strong modal coupling, identification of modes is problematic and labeling is somewhat arbitrary. No attempt has been made to give a complete description of modal coupling in the figures.

illustrating that minimum stiffness is not always the worst case. At 50% stiffness, two whirl modes—antisymmetric wing/pylon chord (q_{f_7}) and symmetric wing/pylon torsion (q_{f_3})—are just barely stable and unstable, respectively.

It is instructive that the predictions in figure 4 were made with the original, uncorrected ATB model. The possibility that reduced control stiffness would destabilize whirl modes was previously known for the steel blades (ref. 7), but it was not considered a significant problem for either the steel blades or ATBs. The potential for unstable blade modes (blade flutter) was not fully appreciated before the present study. Blade flutter does not appear to be a limiting constraint on the steel blades, whose stability boundary is determined by whirl-mode flutter. On the other hand, given their higher mass, solidity, and torsional inertia, the ATBs are strongly susceptible to unstable blade modes, as this report documents.

The problem was exacerbated by control-system characteristics different from those assumed for the ATB design: the effective stiffness varies considerably with collective pitch angle, and flexing in any axis (longitudinal and lateral cyclic plus collective) for either rotor causes first-order perturbations in the inputs of both other axes for that rotor. In contrast, the ATB design assumed uniform, high stiffness in all axes with no coupling.

The present study resulted in several proposed modifications to the ATBs and to the XV-15 to reduce the loads and increase aeroelastic stability margins. Three modifications have already been tested in flight: control-system shims, additional chordwise-balance blade weights, and alternative tips with reduced twist. Their measured effects on loads are documented in reference 6; their predicted effects on stability are documented herein. In addition, flight tests are under way with reduced blade sweep. The effect of sweep on stability is discussed later this report.

This report documents the status of model development at the time the XV-15/ATB was cleared for conversion to airplane mode. It is intended to highlight the most noteworthy issues that arose during the development of the present model in the hope of serving as a spur and a guide to further study. It is not a comprehensive survey of aeroelastic stability throughout the flight envelope, nor is it a catalog of all desired refinements to the CAMRAD model. Only airplane-mode analyses will be discussed; aeroelastic stability in helicopter mode is not an important issue for the ATBs.

This report is divided into two major sections. The first, Improvements to the Baseline Model, discusses the development of the CAMRAD model of the ATBs, including the control-system model, with illustrations of the changes in stability caused by correcting known input errors. The second, Stability Predictions for Flight-Test Configurations, presents stability predictions for the blades as originally flown and with selected combinations of blade configurations and control-system modifications. The CAMRAD model of the XV-15/ATB used for this effort is listed in the appendixes, with notes on some of the more important (or otherwise undocumented) revisions.

The author wishes to thank J. F. Madden for his guidance of the overall effort and for his generous assistance in the revisions to the ATB model. J. R. Gillman, then of the Boeing Helicopter Company, provided the original ATB model plus several crucial revisions, and J. J. Totah was instrumental in setting up CAMRAD with the improved control-system analysis. Wayne Johnson of Johnson Aeronautics provided invaluable assistance in the proper use of CAMRAD plus numerous refinements to the analytical model. The author also acknowledges the contributions of the Rotorcraft Aeromechanics Branch, NASA Ames Research Center, particularly those of R. M. Heffernan, A. A. Swanson, and J. M. van Aken, the cooperation of whom was essential to the creation of a reliable CAMRAD model.

IMPROVEMENTS TO THE BASELINE MODEL

Several different CAMRAD models of the XV-15/ATB were constructed during the course of ATB development. The Boeing C97 model of October 1988 was the most highly developed of those delivered to NASA. It was not developed until after problems with high loads were encountered on the aircraft, and important refinements were made afterward by NASA in cooperation with Boeing. All predictions discussed in this section are based on the C97 rotor model with 1° aft blade sweep, fully twisted tips, no chordwise-balance (tracking) weights, and 20 balance weights (nominal). This is the ATB configuration that was delivered to NASA and is the blade model used for many early analyses. It was selected as a convenient reference against which improvements to the model may be compared.

First to be discussed will be the effects of using additional solution modes in the aeroelastic stability analysis. This does not involve changes to the ATB input data, but is instead an analysis option within CAMRAD. Discussions of changes to the ATB model follow, organized into three subsections: the blade model,

including structural and mass properties; the airframe model, including the drive train; and the control-system model. The last is presented in a separate section because it includes changes both to the model data and to CAMRAD[2] itself. A discussion of the ATB airfoil data is also included. Appendix A is a complete listing of the fully developed CAMRAD model.

The effects of changes to the model are not necessarily additive. Discussion of the fully corrected model is deferred to the section entitled Stability Predictions for Flight-Test Configurations in order to allow more convenient comparisons of configuration differences.

The specified level-flight envelope for the XV-15/ ATB is 260 KEAS and V_{dive} is 300 KEAS, both at sea level (ref. 8); a 20% speed margin for flutter-free operation was also specified, yielding a 360-KTAS stability boundary. Although the ATBs were initially designed to the 300-knot specification (ref. 1), the predicted aerodynamic performance of the final design was slightly higher at 322 knots (ref. 2) as was the predicted stability boundary (unpublished Boeing Helicopter Memorandum 8-7457-1-1057, Sept. 25, 1987). The aeroelastic stability predictions shown in this section are all for airplane mode in level flight, 86% rotor speed (517 rpm), no power or torque limits, and an airspeed range of 250 to 400 KTAS at sea level standard conditions. Power-limited dives were also studied for certain configurations, but level flight with unlimited power is the most convenient reference condition for illustrating the effects of changes in the CAMRAD rotor model.

The discussions that follow emphasize improvements to the model of a given rotor configuration. This report presents results for only a few of the model variations that were analyzed, selected to illustrate the most important differences; only the most important changes to the stability predictions will be explicitly pointed out. The flight conditions presented here were chosen to emphasize the effects of model improvements. Many minor improvements are also pointed out, along with a few areas of continuing research.

C97 Model Predictions

Figure 5 shows the aeroelastic stability predictions made with the original, uncorrected C97 model; it will be used as a baseline reference in the rest of this section. Only a limited number of rotor degrees of freedom were used in the stability solution, equivalent to two bending modes and one pitch/torsion mode per blade, plus axial inflow. The airframe was modeled with rotor-gimbal, drive-train, and rigid-body modes, plus eight flexible-body modes. This was essentially the model used during the design of the ATBs. For all analyses discussed in this report, the "uniform inflow" option in CAMRAD was used with a constant-coefficient approximation for the stability analysis.

Figure 6 shows the predictions with four bending modes and two pitch/torsion modes. The expanded solution does not merely add more modes at higher frequencies: the character of almost all modes is affected. Neither set of predictions shows any instability; however, the drastic changes in the rotor modes (>1/rev) in figure 6 suggest that the reduced dynamic model may be inadequate to predict blade flutter, even though a limited dynamic model would normally suffice to predict whirl-mode flutter (ref. 7).

Blade Model

Possibly the most critical error in the C97 ATB input data was underestimation of the blade torsional (pitch) moment of inertia by almost 45% (0.426 slug·ft^2 actual versus 0.295 slug·ft^2 estimated, not counting the control system). The overlooked inertia comprised many small contributions of secondary structure and hardware (fasteners, etc.) plus the blade cuff (fig. 2). Although the cuff is hollow and very light, most of its mass is distributed well away from the pitch axis and constitutes a large fraction of the total torsional inertia.

Figure 7 shows the stability predictions (eigenvalues) for the full cuff inertia and additional solution modes (four bending and two pitch/torsion modes). The symmetric collective-torsion mode (θ_0) at 3/rev is shifted very close to zero damping (fig. 7(a)), and there is a whirl mode (wing/pylon torsion, q_{f3}) with very low damping just below 1/rev. The antisymmetric collective-torsion mode, coupled with the cross-shaft and first blade-bending modes ($\theta_0/\beta_0/\Psi_I$ in fig. 7(b)), is unstable

[2]Over the years, there have been several different versions of CAMRAD under different names. CAMRAD is the name of the original program developed at NASA Ames Research Center by Wayne Johnson; it is also the generic name for all versions. Some Boeing documents refer to Boeing's implementation of the early version as C-76. CAMRAD/JA is an improved version developed commercially by Johnson Aeronautics (ref. 5). Some of its new features were added to C-76 to create another Boeing version, C-80. C-80 was further expanded to include a full control-system stiffness model, as were some NASA versions of CAMRAD/JA.

between about 260 and 395 KTAS, whereas it was completely stable with the original pitch inertia (fig. 6(b)). Because of the mismodeled engine-shaft influence, the calculated frequency of the antisymmetric collective-torsion/drive-train mode is unreliable, but the decrease in predicted stability is nevertheless significant.

The effect of pitch inertia is not nearly so apparent if CAMRAD is run without the additional solution modes: symmetric collective torsion is shifted down in frequency but is only slightly less stable, and antisymmetric collective torsion shows a trend toward instability without becoming unstable (not shown). Although a limited number of solution modes, as used in the original C97 model, are usually adequate for prediction of whirl flutter, they are not adequate for the prediction of blade flutter.

In the fully corrected model (discussed in the next major section, Stability Predictions for Flight-Test Configurations), more torsional inertia was added to account for control-system mass, which is seen by the blade as increased pitch inertia, but is not separately modeled in CAMRAD. The mean angular position of the pitch horn varies by 30° or more between the helicopter and airplane modes, which significantly changes its effective c.g. (center-of-gravity) offset from the elastic axis. The offset was calculated separately for the airplane and helicopter modes; only the airplane-mode value changed noticeably. The values of blade chordwise stiffness were also changed to reflect the analytical values employed by Boeing (unpublished Boeing Helicopter Company Memorandum D210-12345-1, Rev. B, Dec. 16, 1988). (The original values were based on test data now thought to be inaccurate.)

A compromise had to made in the modeling of the torsional properties (torsional stiffness, moment of inertia, and polar radius of gyration) of the blade cuff. CAMRAD assumes a straight elastic axis that intersects the pitch axis at a given radial location (the feathering axis radial location, RFA). On the ATBs, this geometric intersection is at 0.17 R, well outboard of the hub. CAMRAD does not include torsional properties of the blade inboard of this point in its modal calculations (ref. 5). Most of the blade cuff and all of the effective control-system mass are located inboard of the axis intersection. Because these masses strongly affect blade stability, they were included in the final model by lumping torsional inertia outboard of RFA (at 0.172-0.180 R; see appendix A). A similar compromise was used to model the inertial effects of blade sweep, which are not internally calculated by CAMRAD. A separate research effort is currently under way to evaluate a more physically representative cuff model.

Airframe Model

The most important change made to the airframe model was to the drive train, where the engine-shaft structural damping was severely decreased from 1.0 to 0.01.[3] With this change only, the highly coupled, symmetric collective-torsion/drive-train mode ($\theta_0/\beta_0/\Psi_E/\Psi_S$) is shifted dramatically to a lower level of stability (fig. 8; compare with fig. 6(a)). The effect of reducing engine-shaft damping on rotor-blade stability (fig. 8) is similar to the effect of adding pitch inertia shown in figure 7(a). The blade-lag/drive-shaft mode (β_0/Ψ_E) is less stable, as expected.

The interconnect-shaft damping was correct in the original model, and there is only a quasi-static, antisymmetric degree of freedom for the engine shaft; therefore, no change was expected or seen in the antisymmetric modes (not shown).

Correcting the C97 model with decreased engine-shaft damping, with increased blade-pitch inertia, and with extra solution modes results in an unstable, symmetric collective-torsion blade mode (θ_0) above 325 KTAS (fig. 9). The antisymmetric modes are identical to those in figure 7(b) and thus are not shown. All wing/pylon modes remain stable at all airspeeds, although the stability margin is negligible at 400 KTAS for the symmetric wing chord mode (q_{f3}).

With the corrected engine-shaft damping, no instabilities were seen if the lower number of degrees of freedom in the C97 model was used; only very minor changes were seen when all possible degrees of freedom (five bending and three torsion modes) were used.

The final drive-train model included further changes, particularly for interconnect-shaft stiffness (included in appendix A); they proved not as important as engine-shaft damping. Adding the full drive-train model to the C97 model resulted in negligible change to the predicted stability (not shown).

The final airframe model also includes a revised value for wing/body drag in airplane mode, documented in reference 9 for the steel blades, and verified by more recent steel-blade performance data. (As of this writing, there is no complete set of flight-test performance data for

[3]The larger, incorrect value was apparently a typographical error dating back to an earlier version of the CAMRAD XV-15 model, predating the ATB project.

the ATBs.) Also included are extensive revisions to control gains and offsets plus aircraft c.g. and rigid-body inertias. These changes make little or no difference to stability predictions, except possibly for the effects of small changes in trimmed collective settings.

Control System Model

A tiltrotor requires very large collective pitch changes as the airspeed increases from hover to high-speed, airplane-mode flight. Small-diameter hubs are required for low drag, but long spinners are acceptable. Lateral cyclic is needed only to trim blade flapping, roll control being provided by flaperons in airplane mode and by differential collective in helicopter mode (ref. 10). The design constraints were thus very different for the XV-15 than for a pure helicopter, resulting in an unusual type of rotor-control system.

Figure 10 illustrates the XV-15 rotor-control system. The swashplate has only cyclic motion, and collective control is input by a separate rise/fall collective head above the rotor. The collective head, or spider, is driven by a separate actuator by means of a long tube running through the transmission. Collective and cyclic inputs are mixed by walking beams attached to the spider, with the blade pitch links connecting to trailing pitch horns. In this arrangement, only the collective actuator needs to be capable of a large range of travel. The swashplate tilts but does not translate; it is mounted to the transmission case by a gimbal ring. A conventional, high-rate hydraulic actuator controls longitudinal cyclic; a low-rate, limited-motion actuator controls lateral cyclic. The swashplate and its gimbal, the walking beams, the pitch links, and the pitch horns are all aluminum; the rest of the control system is steel.

The original C97 model assumed uniform, constant control-system stiffness of 13,900 ft·lb/rad for collective, cyclic, and reactionless degrees of freedom. The eigenvalues for stiffness variations are illustrated for the original C97 model in figure 4 (with extra solution modes), and for the model with corrected cuff inertia and engine-shaft damping in figure 11. Several modes are less stable in figure 11 than in figure 4; the most important is the symmetric collective-torsion/drive-train mode ($\theta_0/\beta_0/\Psi_E/\Psi_S$), which has more than doubled in frequency compared to that shown in figure 4(a). This mode shows a sudden decrease in stability above 110% stiffness, and the "pure" (i.e., relatively uncoupled) collective-torsion mode (θ_0) shows an increase in stability at the same stiffness—a classic indication of coalescence. Note also that the corresponding antisymmetric mode ($\theta_0/\beta_0/\Psi_I$) is least stable at almost exactly the nominal control-system stiffness.

Although the simple, constant-stiffness model had been used successfully for analysis of the steel blades, it proved inadequate for analyzing the ATBs because of their higher pitch inertia. Stiffness is different for collective and cyclic motions; in general, it is also different for longitudinal and lateral cyclic. Furthermore, there is crosstalk between the different input axes, caused in part by structural deformation of the inner gimbal ring. Finally, the total stiffness seen by the blade depends on the angle of the pitch horn, varying as $\cos^2\theta_0$. These effects were added to CAMRAD by allowing the specification of a fully coupled control-stiffness matrix. The effects of varying pitch-horn angle and collective-actuator extension were simulated by using a different stiffness matrix for each trim point, with matrices usually calculated for every 5° of pitch-horn angle.

Not all of the needed information was available when the C97 model was first constructed by Boeing; indeed, complete measurements of control-system flexibility were not performed until after the ATBs had begun flight tests. An extensive ground test was required to adequately characterize the system. The matrices used for the predictions shown here are given in appendix B.

The effects of using the full control-system stiffness matrices with the C97 model are shown in figure 12. Additional solution modes are also used, but the original (incorrect) cuff inertia and drive-train model are retained to allow comparison with figure 6. The most dramatic change is seen for the antisymmetric collective-torsion mode, which is heavily coupled with the first bending mode and the drive train and is now unstable above about 312 KTAS ($\theta_0/\beta_0/\Psi_I$ in fig. 12(b)). In contrast, the symmetric collective-torsion mode (θ_0) has become more stable. The antisymmetric predictions remain unreliable because of the drive-train model, but the differences between figures 6 and 12 are nevertheless significant. No instabilities were seen if the limited number of degrees of freedom in the original C97 model was used. Again, limiting the number of degrees of freedom hides certain instabilities.

Airfoil Data

The ATB model was changed in one additional area: the airfoil data. The blades have three different airfoils plus two transition regions. Figure 3 shows the blade planform and actual locations of the different airfoils. The

most inboard segment is the blade cuff,[4] which is tapered in planform and truncated at 78% chord at the root. The truncation is swept to give maximum clearance inboard. (This avoids interference with the conversion-actuator fairing at the wing tip when the rotor is at high collective angles in airplane mode.) The truncation and taper together create the appearance of uniform sweep (fig. 3), but the aerodynamic behavior is more similar to a tapered but unswept cuff. The cuff has a Boeing V43030-1.58 airfoil, which is based on the NACA 430-series cambered airfoil (ref. 3).

The midspan blade segment is a Boeing VR-7 airfoil with a –3° tab. The most outboard segment is a modified Boeing VR-8 airfoil, and the remaining segments are linear transitions between the VR-7 and the other airfoils. For modeling purposes in CAMRAD, the inboard transition region is combined with the cuff airfoil, resulting in four modeled radial segments.

CAMRAD uses C81 tables for aerodynamic data, in which lift, drag, and pitching-moment coefficients are tabulated versus angle of attack for several different Mach numbers from 0 to 1. For the ATBs, tabulated angle of attack covered the full ±180° range, with finer increments near zero angle of attack.

Each airfoil table was constructed by Boeing by splicing two-dimensional wind-tunnel data, taken near zero angle of attack, into theoretical predictions for an angle of attack range of ±180°. The original splicing was discovered to be very ragged, sometimes showing physically unrealistic changes in the aerodynamic coefficients, such as slope reversals at the splice points. Because these errors were only rarely within the angle-of-attack range calculated by CAMRAD, their effects on the aeroelastic predictions were assumed to be negligible and were not explicitly studied. Nevertheless, the data splices were smoothed out by J. Totah for his work reported in reference 6. The resulting C81 tables are given in appendix A. Efforts are being made to further refine the tables, especially for the truncated cuff airfoil.

The original C97 model for the outboard blade sections was further modified by eliminating an offset aerodynamic center (XA < 0). An offset forward of the elastic axis had been used by Boeing to get better loads correlation for helicopter mode, but was considered to be unnecessarily conservative for airplane mode (axial flow). Accordingly, the aerodynamic center offset was set to zero in the final ATB model (see appendix A). An offset was retained at the cuff to compensate for the truncation of the airfoil.

All predictions through figure 12 were made with the original, uncorrected tables and aerodynamic offset at the tips. All predictions that follow were made using the corrected tables and zero offset except where noted.

STABILITY PREDICTIONS FOR FLIGHT-TEST CONFIGURATIONS

The preceding section discussed the most important corrections and refinements to the original CAMRAD model of the ATBs. The following section will discuss the effects of different rotor and airframe configurations on aeroelastic stability as predicted with the improved model.

The ATBs can be tested in several different configurations. They have been flown to date with two different sets of tips and two different settings of blade sweep. They have also been flown with a modified (shimmed) control system and different numbers of chordwise balance (tracking) and rotor balance weights (ref. 6). However, not all possible combinations have been flown; table 1 lists the configurations flown so far. (The chordwise balance was fixed early in the test program at 20 forward (leading-edge) weights; therefore, weight combinations are not listed.)

Table 2 lists the maximum stable airspeeds for each configuration analyzed. The effects on stability of control-system stiffness, tip twist, and blade sweep are discussed individually below, and the effects of modeling an offset aerodynamic center are also summarized. The reader is reminded that predictions of antisymmetric modes are not completely reliable, because of improper computation by CAMRAD of the effects of engine-shaft inertia.

For all analyses in this section, including that shown in table 2, the airspeed range was lowered because of the known instabilities well below 400 KTAS. The rotor speed was reduced to 80% (481 rpm) to more closely match the expected operating condition for the ATBs. (The analyses presented through fig. 12 were initiated before flight tests revealed that the rotor speed for the ATBs could be lowered from the previous nominal value without exciting excessive loads.) The lower rotor speed also more clearly reveals the effects of blade configuration changes.

An additional analysis was performed with full corrections except for the control-system stiffness model, which had uniform stiffness (13,900 ft·lb/rad) and no

[4]This is the "basic" or "baseline" cuff of refs. 1, 2, and 4.

cross-coupling. The blade model had 1° aft sweep and twisted tips with zero aerodynamic-center offset. As expected, many minor changes in the eigenvalues were noted with respect to those discussed in the preceding section, but there were no important changes in the character of the instabilities. At 80% rpm, the symmetric stability boundary was 305 KTAS, but the antisymmetric boundary was only 239 KTAS. These values were both about 20 knots higher at 86% rotor speed (figs. 7(b) and 9).

Blade Configurations

The ATBs were delivered to NASA with two sets of tips, each geometrically similar but with different twist. All tips physically begin at 0.877 R (fig. 3). The original, twisted tips[5] have about 5° of twist, which simply continues the blade twist to the end. The alternative tips have zero twist outboard of 0.877 R, both aerodynamically and structurally. The twisted tips are expected to give better performance at extreme operating conditions, specifically at high C_t/σ. At low and moderate C_t/σ in helicopter mode, however, the twisted tips experience negative angles of attack, worsening performance and loads. Because adverse loads in helicopter mode were the immediate problem in initial ATB flight tests, maximum theoretical performance was deliberately sacrificed in exchange for reduced loads by substituting untwisted tips. See reference 6 for loads predictions for the two tip configurations.

(References 1 and 4 report whirl-stand test results for two further tip configurations: square and swept. No stability analyses were performed for those tips because complete, flightworthy sets of them do not exist for both rotors, and there are at present no plans for flight tests.)

The sweep of the blade aerodynamic center may be varied with respect to the pitch axis by using different eccentric bushings with the blade attachment pins (fig. 2). To date, only 1° aft sweep and 0° sweep have been tested.

Figure 13 shows the eigenvalues for the updated ATB model with full control-system stiffness effects included. The blade model is for 1° sweep and twisted tips, the first configuration flown (and for ease of comparison, the closest match to fig. 9). The symmetric collective-torsion mode (θ_0) is now completely stable. Compare figure 13(a) with figure 9, and note that the drive-train coupling has shifted to the less stable mode ($\theta_0/\beta_0/\Psi_E/\Psi_S$ in fig. 13(a)). The stability of the antisymmetric collective-torsion/drive-train mode ($\theta_0/\beta_0/\Psi_I$) is improved by nearly 50 knots; compare figures 13(b) and 7(b) (keep in mind the difference in plotted airspeeds). At 86% rotor speed, the symmetric and antisymmetric instabilities occur at 393 and 319 KTAS—increases of 70 and 90 knots, respectively, compared with the original control-system model.

Comparing figure 13 and figure 12 illustrates the effects of improving the blade model, given the same control-system model. For the symmetric case, the stability of the collective-torsion/drive-train mode ($\theta_0/\beta_0/\Psi_E/\Psi_S$) is drastically reduced, but never to the point of instability. For this mode in figure 13(a), collective torsion (θ_0) is only weakly coupled to first blade bending (β_0) and to the drive train (Ψ_E/Ψ_S). For the antisymmetric case, the stability boundary is virtually unchanged.

Close examination of figure 13 illustrates one of the difficulties of the present control-system model: the values in the stiffness matrix depend on the collective position, but CAMRAD, as modified, does not automatically adjust the matrix as it converges on a new trim setting. The matrix must be specified in advance and the trim manually checked afterward for consistency. The lack of a fully automated trim routine in CAMRAD imposes a practical limit on the resolution of the stiffness values used for each trim point. This limits in turn the accuracy of the trimmed control settings, which influence the stability predictions.

The effect of the resolution limit can be seen most clearly in the second-bending/drive-train modes just above 2/rev (β_2/Ψ_E and β_2/Ψ_I in figs. 13(a) and 13(b), respectively). Although the airspeed increments are a constant 25 KTAS, the eigenvalues are not evenly spaced and tend to group into pairs. Each pair corresponds to a different stiffness matrix, with a 5° increment in collective between each matrix. The spacing could be improved by using more stiffness matrices at finer collective increments, but the resolution effects seen here are smaller than the effects of known uncertainties in the measurements of control-system stiffness.

Control-System Modifications (Shims)

Because lateral cyclic is needed only to trim blade flapping with airspeed, it was possible to temporarily stiffen the swashplate by locking the inner gimbal ring in place with shims wedged between it and the transmission case (fig. 14). The shims transferred bending loads from the longitudinal-cyclic gimbal bearings directly to the

[5]These are the "basic" or "baseline" tips of references 1, 2, and 4.

transmission case, reducing warping of the inner gimbal. This fixed lateral cyclic at a single compromise setting of 0°, adequate for research flights. The swashplate remained free to tilt for longitudinal cyclic.

More than one shim thickness is possible, each thickness corresponding to a different lateral cyclic setting. The allowable range is 0° to –4°; only the 0° setting has been flown. All shims would have similar effects on control-system stiffness, hence on aeroelastic stability. Accordingly, stability analyses were done for only two basic control-system configurations: with and without 0° shims.

Control-system stiffness matrices with and without shims are listed in appendix B. The effects of control-system stiffness on blade loads with and without shims are reported in reference 6.

Although the blade configuration with shims and twisted tips was flown only briefly in helicopter mode, it was analyzed for airplane-mode stability to assess the effects of shims separately from the effects of tips. The eigenvalue plot is given in figure 15. The shims destabilize the collective-torsion/drive-train mode in the symmetric case ($\theta_0/\beta_0/\Psi_E/\Psi_S$) and stabilize it in the antisymmetric case($\theta_0/\beta_0/\Psi_I$); compare figure 15 and figure 13. Modes above about 6/rev are nearly identical. Shims increase the maximum stable airspeed very slightly from 308 KTAS to 312 KTAS, but the boundary is now set by a symmetric instability. The net airspeed improvement is insignificant in light of the limited resolution of the stiffness matrices, but the shift in the limit from an antisymmetric to a symmetric mode is important. The key payoff is in reduced control-system loads, as reported in reference 6.

Table 3 lists the frequencies of selected blade modes for the ATBs with 1° blade sweep and twisted tips. Values are given for three control-system stiffness models: constant stiffness (no stiffness matrix), fully coupled, and shims. The values are typical for all other XV-15/ATB configurations; the exception is collective torsion (θ_0). That mode is very sensitive both to the configuration and to the accuracy of the CAMRAD model. When the fully coupled matrix and then the shim matrix are added to the model, each matrix causes a 13% increase in collective-torsion frequency.

Because the critical aeroelastic instability for the ATBs has been found to be a flutter phenomenon, it is important to point out the crucial influence of the bending/torsion frequency ratios. Classic flutter theory holds that coincident or coalescent wing-bending and torsion frequencies produce minimum flutter airspeeds. The XV-15/ATB is a rigid (gimballed) rotor with highly twisted blades. Blade-bending modes—both flap and lag—are strongly coupled with each other and with the drive train. With the XV-15/ATB rotor system, the relatively high blade-torsional inertia produces torsion-mode frequencies close to the collective-rotor/drive-train natural frequencies. The frequency shift in the collective-torsion mode (table 3) is the major cause of the changes in stability boundaries between figures 13 and 15. The difference between predicted symmetric and antisymmetric stability is caused primarily by the difference in the critical rotor/drive-train natural frequencies between the two cases.

Zero-Twist Tips

The second shimmed configuration flown had zero-twist tips. The intent was to reduce loads as much as possible for the existing blade sweep (1° aft). This configuration was the first to convert fully to airplane mode.

The eigenvalue plot of symmetric modes is almost identical to that for the twisted tips shown in figure 15(a) (hence no separate plot is shown). The major difference is a 10-knot reduction in the maximum stable airspeed, determined by the collective-torsion/drive-train mode as before. The antisymmetric modes also show only minor differences from the twisted-tip configuration, all remaining stable.

Zero-Sweep Blades

For the next flight-test configuration, the blade sweep was set to 0°; the shims and zero-twist tips were retained. This configuration was expected to yield the maximum possible loads reduction. The eigenvalues are similar to those shown in figure 15 (hence no separate plots are given). The stability of the collective-torsion/drive-train mode is slightly reduced for both the symmetric and antisymmetric cases, with a maximum stable airspeed of 293 KTAS for the symmetric case greater than 350 KTAS for the antisymmetric case. As would be expected with reduced blade sweep, whirl-mode stability boundaries are reduced for both cases but remain above 350 KTAS at full (unlimited) power. Whirl-mode stability would be reduced in a power-off dive (windmill state).

Aerodynamic Center Offset

All results reported above are based on models with no offset to the aerodynamic centers of the blades (except at the cuffs). The improved model was analyzed with the offset used in the C97 model (given in appendix A). For the first configuration discussed—full stiffness matrices, 1° sweep, and standard tips—adding the offset had a negligible effect on antisymmetric modes. The effect on the stability boundaries of symmetric modes could not be precisely determined because those modes were always stable, but the changes appeared to be very slight. For the other configurations, all of which had the shimmed control system, the stability boundary of the symmetric collective-torsion/drive-train mode was reduced by 20 knots. Reduced stability margins were also seen for the corresponding antisymmetric mode, but it always remained stable up to 350 KTAS. For the least stable configuration, that with zero sweep, the aerodynamic offset produced unstable whirl modes. The symmetric wing-chord mode was unstable above 340 KTAS, and the antisymmetric wing beam-bending mode was unstable above 349 KTAS. The maximum stable airspeed remained limited by blade flutter.

CONTINUING EFFORTS

Modifications in addition to those already flight tested (blade sweep, tip twist, and shims) are also being studied. Among them are leading-edge weights to increase blade-mode stability, torsional absorbers for the blades to detune the resonant response, and further stiffening of the control system to increase its natural frequency. The goal is to reduce blade loads below those already achieved while extending aeroelastic stability out to the original design requirement of 360 knots (300 KTAS level flight plus a 20% margin). CAMRAD is being used to analyze these design variations for both stability and loads.

As a fundamental part of this effort, the baseline CAMRAD model of the ATBs and XV-15 is continually being improved. For example, the aerodynamics of the truncated blade cuff are known to be poorly modeled. The consequences appear to be negligible, based on preliminary analyses of new aerodynamic data, but this has yet to be completely confirmed. The wing/pylon structural modes, as modeled in NASTRAN, are also considered to be of questionable accuracy, as are the estimates of aerodynamic damping for those modes. These inputs are critical for proper analysis of whirl-mode flutter. It is planned to update the structural model with the results of a ground vibration test of the entire XV-15. Modifications to CAMRAD that will allow it to internally calculate the control-system stiffness matrices and to improve the drive-train model are in progress.

CONCLUSIONS

Correcting the CAMRAD model of the XV-15 Advanced Technology Blades reduced the predicted aeroelastic stability boundary from over 400 knots to just over 300 knots (true airspeed). The limiting instability was always a highly coupled collective-torsion/drive-train mode. Two errors contributed to this gross misprediction: the blade-pitch inertia was initially set too low, and the engine-shaft damping was too high. It was also discovered that the number of degrees of freedom used in the original analysis was inadequate to reveal the critical instability.

Another major improvement was better modeling of the control-system stiffness. When modified with a fully cross-coupled stiffness matrix, CAMRAD predicted a stability boundary of 308 KTAS for the baseline rotor model.

Modifications were made to both the airframe and the rotors in the course of flight testing. The stiffness of the XV-15 control system was increased by adding shims between the inner gimbal ring and the transmission case. This raised the blade-pitch-mode frequency, which significantly reduced loads, but had only a slight benefit on the stability of the blade modes. The ATBs were modified with zero-twist tips and zero sweep to further reduce loads. Both changes were predicted to reduce the stability boundary by 10 knots each. Whirl-mode stability remained acceptable in all cases.

An offset aerodynamic center at the blade tips was eliminated from the model. No effect on stability was seen with the full model of the unmodified aircraft control system, but an almost uniform 20-knot reduction in stability was seen with the shimmed control system. The validity of the aerodynamic offset has not been confirmed, and the predictions made without it are presently considered to be more reliable.

Because of limitations in CAMRAD's calculation of the effects of engine-shaft inertia on rotor stability, no results concerning antisymmetric modes can be considered final. Nevertheless, CAMRAD adequately reveals the relative benefits of the different changes in the model and in the aircraft and rotors.

APPENDIX A: THE CAMRAD MODEL OF THE XV-15/ATB

Airframe/Rotor Model

The namelist input data for the XV-15/ATB are given below for airplane mode. The nominal blade configuration is 1° sweep and fully twisted tips, with Boeing's aerodynamic-center offsets. Alternative data for 0° sweep, zero-twist tips, and zero offset are included as comment fields. Other comments note changes to the C97 model, several of which were suggested by Wayne Johnson. Page numbers refer to the CAMRAD/JA User's Manual (ref. 5).

The namelists have been simplified and reformatted for publication. Certain unused inputs (identically equal to zero) have been deleted. CAMRAD can regenerate namelists from binary data, and most of the data given below have been left in the default output format. The number of significant figures is, therefore, neither consistent nor meaningful, being determined by FORTRAN output conventions and the data-storage specifications of the computer code.

CAMRAD/JA users should be aware that there are two different XV-15 aircraft. Only aircraft S/N 703, operated by NASA, has been flown with the ATBs. Both aircraft have "lateral cyclic (trim) bias" (CNTRLZ(2) and CNTRLZ(5)), effective in helicopter mode, and "longitudinal cyclic (trim) bias" (CNTRLZ(3) and CNTRLZ(6)), effective in airplane mode. Aircraft S/N 702, operated by Bell, also has a "flapping controller" that uses lateral cyclic in airplane mode. The published literature does not consistently distinguish between these three trim inputs; any of them may be referred to as "flapping control." Users should also be aware that GTRS (ref. 11) uses a reference wing area of 181 ft^2, whereas the standard CAMRAD model uses 169 ft^2.

CAMRAD namelist input for the XV-15/ATB in airplane mode
(page numbers are those in ref. 5, vol. II; additional comments are in brackets):

```
$NLTRIM
! Case description (p. 100)
TITLE  = 'XV-15/ATB: 0-DEG PYLONS, AEROELASTIC STABILITY ANALYSIS',
CODE   = 'FLUTTER',
OPUNIT = 1,     ANTYPE = 1,2*0,    OPREAD = 10*1,
NPRNTI = 1,     TRACE  = 0,        DEBUG  = 24*0,    DBTIME = 3*0,
! Operating conditions (p. 103) [80% x 601 rpm:]
VKTS   = 250.0, VEL    = 0.00,  VTIP = 0.00,  RPM = 480.80, AFLAP = 0.0,
OPDENS = 1,     ALTMSL = 0.00,  TEMP = 0.00,  DENSE = 0.00,
OPGRND = 0,     HAGL   = 0.00,
! Aircraft description (p. 104)
NROTOR = 2,     OPENGN = 0,
DOF    =    3*1,7*0,  1,4*0,  1,
            3*1,7*0,  1,4*0,  1,
            42*0,
DOFT   =    2*1, 2*0, 2*1, 2*0,
! Motion analysis (p. 105)
MPSI   =  24,     MHARM  = 2*2,    MHARMF = 2*0,
MPSIR  =  24,     MREV   = 1,
ITERM  =  20,     EPMOTN = 0.01,
ITERC  =  20,     EPCIRC = 0.001,
! Wake analysis (p. 106)
LEVEL  =  2*0,    ITERU = 1,     ITERR = 0,    ITERF = 0,
! Trim analysis (p. 107)
OPTRIM = 7,     MTRIM  = 40,
MTRIMD = 20,    DELTA  = 0.5,  OPTIDR = 1,   ALPHA = 0.5,
FACTOR = 0.5,   EPTRIM = 0.005,
OPGOVT = 3,     OPWT2T = 1,
! Initial control settings (p. 110)
COLL   =  23.7,    LATCYC = 0.89,    LNGCYC =  0.62,
PEDAL  =  0.00,    THROTL = 0.00,    APITCH = -1.72,
AROLL  =  0.00,    ACLIMB = 0.00,    AYAW   =  0.00,    RTURN =  0.00,
CTTRIM =  0.00,    CPTRIM = 0.00,    CXTRIM =  0.00,    XTRIM =  0.00,
CYTRIM =  0.00,    BCTRIM = 0.00,    BSTRIM =  0.00,
! Trim output control (p. 111)
NPRNTT = 0,     NPRNTP = 0,     NPRNTL = 0,
NTFILE = 0,     NEFILE = 0,
$END

$NLRTR
! Rotor configuration (p. 121)
TITLE='XV-15/ATB: 20 BALANCE WTS, 20 TRACKING WTS, 110% ITHETA (26 JUNE 1989)',
TYPE    = 'RGHT',
```

```
RADIUS  = 12.5,    NBLADE  = 3,       SIGMA   =  0.103,   ROTATE  = 1,
VTIPN   = 600.0000,
! Aerodynamic model (p. 123)
BTIP    =  0.995,  OPTIP   = 1,
! RGMAX=0 per W. Johnson (C97 model had 0.85):
LINTW   =  0,      TWISTL  =  0.00,   RGMAX   =  0.00,
OPUSLD  =  2,      OPCOMP  =  1,
OPREYN  =  0,      EXPRED  =  0.00,   EXPREL  =  0.00,
OPCFD   =  0,      LDMCFD  =  3*0,
! Stall model (p. 125)
OPSTLL  =  1,      OPYAW   =  0,
ADELAY  =   15.00000,                 AMAXNS  =  4.000000,
TAU     = 3*-1.00, PSIDS   = 3*15.00,
ALFDS   = 3*15.00, ALFRE   = 3*12.00,
CLDSP   =  2.00,   CDDSP   =  0.00,   CMDSP   = -0.65,
! Inflow model (p. 126)
INFLOW  =  1, 5*0, KHLMDA  =  1.200,  KFLMDA  =  2.000,
OPFFLI  =  2,      KXLMDA  =  0.00,   KYLMDA  =  0.00,
! FXLMDA=1.0 per W. Johnson (C97 model had 1.5):
FXLMDA  =  1.0,    FYLMDA  =  1.0,    FMLMDA  =  1.0,
KINTH   =  0.00,   KINTF   = -0.085,
KINTWB  =  1.50,   KINTHT  =  1.80,   KINTVT  =  0.00,
FACTWU  =  0.2,    OPTZT   =  0,      CTSTZT  =  0.00,
! Dynamic model -- bending and torsion modes (p. 128)
HINGE   =  1,      RCPL    =  1.0,
EFLAP   =  0.0,    ELAG    =  0.0,    KFLAP   =  0.00,    KLAG    =  0.00,
TSPRNG  =  0.00,   RCPLS   =  0.00,   RFA     =  0.17,
MRB     =  50,     MRM     =  50,     EPMODE  =  0.2,
NONROT  =  0,      NCOLB   =  8,      NCOLT   =  4,
! NUGC and NUGS are based on measured Kg = 290 ft-lb/deg:
NUGC    =  1.0200,      NUGS    =  1.0200,
GDAMPC  =  25.0,        GDAMPS  =  25.0,
! Dynamic model -- control system (p. 129)
TDAMP0  =  0.00,   TDAMPC  =  0.00,   TDAMPR  =  0.00,
WTIN    =  1,
FT0     =  5.40,    FTC    =  5.40,    FTR    =  5.40,
! Nominal control-system stiffness values:
KT0     =  13900.0, KTC    =  13900.0, KTR    =  13900.0,
LDAMPC  =  0.00,   LDAMPM  =  0.00,   LDAMPR  =  1.00,
! Dynamic model -- blade properties (p. 130)
GSB     =  10*0.01, GST    =  5*0.01,
MBLADE  =  -1.0,   MASST   =  0.00,   XIT     =  0.00,
! Dynamic model -- pitch-bending coupling (p. 131)
! Design drawings show PHIPH=-16.54, but test results agree better
! with the higher value in the C97 model:
KPIN    =  2,      PHIPH   =  -20.50, PHIPL   =  0.00,
```

```
! RPB per W. Johnson's steel-blade model (C97 model had 0.06):
RPB     =  0.091,  RPH     =  0.017,  XPH     =  0.063,
ATANKP  =  10*0.00,       DEL3G   =  -15.00000,
! Dynamic model -- root geometry
ZFA     =  0.00,   XFA     =  0.00,   CONE    =  1.5,
! Design drawings define 1-degree nominal sweep in a different axis system:
DROOP   =  0.4617, SWEEP   =  0.887,
! DROOP=0.0 and SWEEP=0.0 for 0-degree sweep; see also ITHETA.
FDROOP  =  0.00,   FSWEEP  =  0.00,
OPHVIB  =  3*1,    FACTM   =   0.2,
! Blade section aerodynamic characteristics (p. 133)
MRA     =  20,
RAE     =  0.1670,  0.2400,  0.3000,  0.3500,  0.4000,  0.4500,
           0.5000,  0.5500,  0.6000,  0.6500,  0.7000,  0.7500,
           0.8000,  0.8400,  0.8800,  0.9200,  0.9500,  0.9700,
           0.9800,  0.9900,  1.0000,  10*0.0000,
CHORD   =  2*0.1333000, 7*0.1347000,  0.1337000,  0.1233000,  0.1099000,
             0.1022000,  9.7099997E-02,  9.0800002E-02,  8.3300002E-02,
         7.1699999E-02,  5.7300001E-02,  4.7699999E-02,  3.8100000E-02,
         10*0.0000,
TWISTA  =  25.5000,  20.7500,  18.6250,  15.8750,  13.5000,  11.2500,
            9.000,    6.8750,   4.8750,   2.8125,   0.9444,  -0.8333,
           -2.3542,  -3.7708,  -5.2159,  -6.5000,  -7.4375,  -8.0000,
           -8.3500,  -8.7000,  10*0.0000,
! For zero-twist tips, TWISTA(14)=7*-3.771; see also TWISTI.
THETZL  = 30*0.00,
XA      = -1.5500000E-02, -4.8000002E-03,  7*0.0000000E+00, -1.3000000E-04,
          -4.9000001E-04, -8.8000001E-04,   -1.3300000E-03, -2.0399999E-03,
          -2.6300000E-03, -3.5000001E-03,   -4.1600000E-03, -4.1299998E-03,
          -3.9599999E-03, -4.3799998E-03, 10*0.0000000E+00,
XAC     = -1.5500000E-02, -4.8000002E-03,  7*0.0000000E+00, -1.3000000E-04,
          -4.9000001E-04, -8.8000001E-04,   -1.3300000E-03, -2.0399999E-03,
          -2.6300000E-03, -3.5000001E-03,   -4.1600000E-03, -4.1299998E-03,
          -3.9599999E-03, -4.3799998E-03, 10*0.0000000E+00,
! XA(3)=18*0.0 and XAC(3)=18*0.0 for zero aerodynamic offset.
ASWEEP  = 30*0.00,
! C97 model had MCORRL, MCORRD, & MCORRM(16:20)=0.965; all =1.0 per W. Johnson:
MCORRL  = 20*1.000, 10*0.000,
MCORRD  = 20*1.000, 10*0.000,
MCORRM  = 20*1.000, 10*0.000,
DELCD   = 30*0.00,  DELCM  = 30*0.00,  RETAB1  = 30*0.00,
! Blade section inertial and structural characteristics (p. 134)
MRI     =  51,
RI      =  0.000,  5.0000001E-02,  5.2000001E-02,  0.100,  0.102,
           0.120,  0.122,  0.130,  0.132,  0.160,  0.170,  0.172,
           0.178,  0.180,  0.200,  0.230,  0.250,  0.273,  0.300,
```

```
          0.325,  0.400,  0.508,  0.550,  0.600,  0.660,  0.690,
          0.778,  0.845,  0.860,  0.862,  0.865,  0.867,  0.879,
          0.881,  0.883,  0.885,  0.893,  0.895,  0.900,  0.902,
          0.910,  0.912,  0.925,  0.935,  0.940,  0.950,  0.960,
          0.970,  0.975,  0.985,  1.000,
TWISTI  = 10*0.0000, 2*27.5000,   26.9600,   26.8800,   25.5500,
           23.8200,   22.7500,   21.4300,   19.9000,   18.6400,
           14.9900,    9.7300,    7.9300,    5.9300,    3.5000,
            2.1800,   -0.9293,   -3.2330, 2*-3.6300,   -3.8580,
           -3.8610,   -4.4100,   -4.4500,   -4.5580,   -4.5610,
           -4.9160,   -4.9190,   -5.1640,   -5.1680, 2*-5.9000,
           -6.2200,   -6.5100,   -6.6500,   -7.0200,   -7.3900,
           -7.7700,   -7.9500,   -8.2900,   -8.8000,
! For zero-twist tips, TWISTI(32)=20*-3.86; see also TWISTA.
MASS    =  2*2.14059,  6*1.94924,  3*1.53411,   0.39462,   0.54399,
            0.56657,    0.58895,    0.49981, 3*0.51846,   0.27825,
            0.25177,    0.20887,    0.20141,   0.19395,   0.18649,
            0.16188,  2*0.12682,    0.12682,   0.15345,   0.19339,
            0.22002,    0.379796,   0.39268,   0.39181,   0.39094,
            0.38747,    0.38661,    0.38444,   0.35300,   0.23500,
            5*8.9520E-02, 7.8330003E-02,  6.7139998E-02,
            6.15400E-02,  5.2220002E-02,  3.7300002E-02,
! XI(11:18) was increased to reflect cuff mass and pitch horn (per J. Madden):
XI     = 11*0.0,  5*0.006536,  0.00893, 0.00513,  5.1299999E-03,  1.340E-03,
 1.9799999E-03,  2.5500001E-03,  2.6700001E-03,  2.7999999E-03,
 2.8400000E-03,  2.8599999E-03,  2.6700001E-03,  2.0099999E-03,
 0.00187,     0.001808,    0.001607,    0.001514,    0.001229,   0.0015245,
 0.0021435,   0.002765,    0.005279,    0.005915,    0.00752,
 7.7999998E-03,  8.9699998E-03,    9.4699999E-03,    1.107E-02,  1.213E-02,
 1.267E-02,       1.060E-02,         8.5300002E-03,  4*6.4699999E-03,
XC       = 16*0.0000000E+00, -9.1429998E-04, -1.9660001E-03, -3.1999999E-03,
-3.3980000E-03, -3.9940001E-03, -4.8509999E-03, -1.4149999E-03, -1.1000000E-03,
-7.2220003E-04, -5.3329999E-04, -2.9330000E-03, -3.5450000E-03, -3.6859999E-03,
-3.6960000E-03, -3.7330000E-03, 10*1.7330000E-03, 2*2.5330000E-03,
 2.6070001E-03,  4.8130001E-03,    6.3330000E-03,   5.9300000E-03,
 5.3599998E-03,  5.5499999E-03,  2*6.4699999E-03,
KP2      = 2*1.5599999E-04,  1.110E-04, 2*1.130E-04, 3*1.150E-04,
 1.1300000E-04,  1.1500000E-04,  1.1600000E-04,  2.4600001E-04,  1.9200001E-04,
 1.8400000E-04,  1.7900000E-04,  2.8000001E-04,  3.8499999E-04,  4.4800001E-04,
 5.3899997E-04,  7.3799997E-04,  8.2199997E-04,  9.3699998E-04,  9.2999998E-04,
 9.9900004E-04,  1.0350000E-03,  1.1820000E-03,  6.5599999E-04,  4.4700000E-04,
 0.0004007,   0.0003374,   0.0002751,   0.0002446,   0.0001576,  0.0001517,
 0.0001486,   0.0001446,   0.0001302,   0.0001265,   0.0001173,  1.2800000E-04,
 1.9599999E-04,  5.3800002E-04,  5.2200002E-04,  5.0400000E-04,  4.9499999E-04,
 4.7599999E-04,  4.4500001E-04,  3.9400000E-04,  3.8600000E-04,  1.8400000E-04,
 6.7000001E-05,
```

```
 EIZZ     = 2*3583000., 2*1389000., 2*1597000., 3*3333000., 4*1090300.,
             2319000.,   2817000.,   1013000.,    859700.0,   651400.0,
              407200.0,   307300.0,   260400.0,   181300.0,   172100.0,
              159700.0,   113700.0,    93060.00,   50000.00,   36810.00,
               33260.00,   33130.00,   32360.00,   32330.00,   29510.00,
               29310.00, 2*28960.00, 2*27080.00,   25760.00,   25560.00,
               23890.00,   23680.00,   21040.00,   19170.00,   18240.00,
               16320.00,   14440.00,   12570.00,   11670.00,    9792.000,
                6944.000,
 ! Chordwise stiffness values are based on Boeing analysis, not test data:
 EIXX     = 2*2903000., 2*1389000., 2*1597000., 5*3333000., 2986000., 2*5347000.,
             6258000.,   3979000.,   3882000., 4310000.,   4812000.,
             4658000.,   4194000., 2*3583000., 3326000.,   3229000., 3125000.,
             1049000., 13*722000.,    693000.,  687000.,    648000.,  619000.,
             604000., 542000., 479000., 417000., 358000., 240000., 49000.,
 ! ITHETA(12:14) was revised to include cuff inertia (per J. Gillman)
 ! plus an extra 10% of total inertia for controls (per J. Madden):
 ITHETA   = 11*0.00000,  0.327745, 0.776045, 0.925475,
  1.6480001E-02,  2.1890000E-02,  3.1160001E-02,  3.6300000E-02,  4.3660000E-02,
  3.2090001E-02,  3.2320000E-02,  3.0579999E-02,  2.9270001E-02,  3.0290000E-02,
  3.0160001E-02,  2.9880000E-02,  1.3000000E-02,  8.8600004E-03,  7.9300000E-03,
  0.008089,       0.008312,       0.008461,       0.009354,       0.009309,
  0.009071,       0.008833,       0.007881,       0.007643,       0.007048,
  7.0799999E-03,  7.1999999E-03,  7.5200000E-03,  7.3000002E-03,  7.0500001E-03,
  6.9200001E-03,  6.6700000E-03,  5.4400000E-03,  4.1299998E-03,  3.7100001E-03,
  1.5000000E-03,  3.9000000E-04,
 ! For zero-degree sweep, ITHETA(12)=0.31371, ITHETA(13)=0.71989,
 ! and ITHETA(14)=0.85528; see also DROOP and SWEEP.
 GJ       = 11*2569000.,    581300.0,   554540.0,   550500.0,   482300.0,
             4*335400.0, 3*197900.0, 3*137500.0,  2*81940.00, 2*28470.00,
                25600.00, 2*24800.00,   22100.00,   21900.00, 2*21600.00,
                19800.00,   19700.00,   18500.00,   18300.00,   16700.00,
                16400.00,   12500.00,    9720.000,   8330.000,   5560.000,
                 4500.000,   3440.000,   2920.000,   1860.000,    278.000,
 $END

[$NLWAKE not used for stability analysis]

[Rotor no. 2 is the same as rotor no. 1 except TYPE='LEFT' and ROTATE=-1.]

 $NLBODY
 ! Aircraft configuration (p. 143)
 TITLE    = 'XV-15/ATB: 0-DEG PYLONS (14 SEPTEMBER 1989)',
 CONFIG   =   3,
 WEIGHT   =   13000.,
 IXX      =   50950.,  IYY =  20348.,     IZZ = 67168.,
```

```
IXY     =       0.,     IXZ =   1076.,     IYZ =     0.,
TRATIO  =     1.0,
ASHAFT  =  2*0.00,  ACANT   =  2*-1.00, ATILT  =   0.00,
HMAST   =  4.6670,
DPSI21  =    0.00,  CANTHT  =  0.00,    CANTVT  =   0.00,
FSCG    =   24.74,  BLCG    =  0.00,    WLCG    =   6.069,
FSR1    =    25.0,  BLR1    =  16.083,  WLR1    =   8.333,
FSR2    =    0.00,  BLR2    =  0.00,    WLR2    =   0.00,
FSWB    =   24.26,  BLWB    =  0.00,    WLWB    =   8.00,
FSHT    =   46.67,  BLHT    =  0.00,    WLHT    =   8.58,
FSVT    =   47.50,  BLVT    =  0.00,    WLVT    =   9.64,
NPOFF   =       1,
FSOFF   = 20*0.00,  BLOFF   = 20*0.00, WLOFF   = 20*0.00,
! Aircraft elastic modes (p. 146)
NEM     =           8,
QFREQ   =     3.48,      6.28,     8.01,     14.09,
              6.06,      7.77,     7.21,     18.31,        22*0.0,
QMASS   =  228.995,   213.121,   76.233,    14.672,
             13.446,    17.431,   12.867,    34.490,       22*0.0,
QDAMP   = .03,  .05,  .05,  .02,  .05,  .05,  .05,  .02,   22*0.0,
DOFSYM  = 4*1, 4*-1, 22*0,
KPMC1   = 30*0.00, KPMS1 = 30*0.00, KPMC2 = 30*0.00, KPMS2 = 30*0.00,
ZETAR1  =  .048487,   -.052894,   -.963608,
          -.641698,    .931786,    .387508,
           .213548,   -.294398,    .715103,
          -.080248,   -.245880,   -.029311,
          -.047290,    .158571,   -.156655,
          -.018050,    .048239,    .317394,
          -.103339,    .008216,   -.155353,
          -.008358,   -.160424,    .017989, 66*0.0,
ZETAR2  =  .048487,    .052894,   -.963608,
          -.641698,   -.931786,    .387508,
           .213548,    .294398,    .715103,
          -.080248,    .245880,   -.029311,
           .047290,    .158571,    .156655,
           .018050,    .048239,   -.317395,
           .103339,    .008216,    .155353,
           .008358,   -.160424,   -.017989, 66*0.0,
GAMAR1  =  -.171719,    .019668,  -.000973,
           -.040915,   -.154005,   .234420,
           -.042429,   -.281872,  -.078687,
            .080573,    .010099,  -.083472,
           -.037836,    .031106,   .023285,
           -.006231,   -.118944,   .022426,
            .036076,    .068589,   .018018,
            .225375,   -.023243,  -.122466,  66*0.0,
```

```
GAMAR2  =   .171719,   .019668,   .000973,
            .040915,  -.154005,  -.234240,
            .042429,  -.281872,   .078687,
           -.080573,   .010099,   .083472,
           -.037836,  -.031106,   .023285,
           -.006231,   .118944,   .022426,
            .036076,  -.068589,   .018018,
            .225375,   .023243,  -.122466,  66*0.0,
QDAMPA  =   267.2,    0.814,    4.009,    2.882,
            4.909,     1.53,   0.7353,   50.595,  22*0.0,
QCNTRL  =   62.19,  -42.78,  2*0.00,     1.55,    54.14,    2*0.00,
            -3.39,   25.75,  2*0.00,  -70.32,  -33.48,    2*0.00,
           2*0.00,  -70.10,  -52.62,  2*0.00,   28.50,  -219.29,
           2*0.00,   -0.95,   42.19,  2*0.00,  -70.02,    31.01,      88*0.00,
! Auxiliary forces
NAF     = 0,
FSAF    = 5*0.00, BLAF    = 5*0.00, WLAF    = 5*0.00,
AZAF    = 5*0.00, ELAF    = 5*0.00, AUXSYM  = 5*0,
ZETAAF  = 450*0.00,
! Control system; [revised per refs. 10 and 11]:
TCIN    =  0,    TCNTRL  = 80*0.00,
K0CFE   =  0.00, KCCFE   = -0.121, KSCFE   =  0.00, KPCFE   =  0.00,
PCCFE   =  0.00, PSCFE   =  0.00,  PPCFE   =  0.00,
KF0CFE  =  0.00, KR0CFE  =  0.00,  KFCCFE  =  0.00,
KRCCFE  =  0.00, KFSCFE  =  0.00,  KRSCFE  =  0.00,
KFPCFE  =  0.00, KRPCFE  =  0.00,
PFCCFE  =  0.00, PRCCFE  =  0.00,  PFPCFE  =  0.00, PRPCFE  =  0.00,
KFCFE   =  0.00, KECFE   =  4.167, KACFE   =  3.93,
KRCFE   =  8.00, KTCFE   =  6.3,
KTTCFE  =  0.00, KATCFE  =  0.00,  KAPCFE  =  0.00,
CNTRLZ  =  21.3,0.0,-1.5, 21.3,0.0,-1.5, 0.0,-2.0,3*0.0,
FORCEZ  =  5*0.00,
! Aircraft aerodynamic characteristics (p. 150)
OPBAT   =   0,     OPDRV   =  0,       OPDRVU  =   0,
IWB     =   3.5,   IWBD    =  3.5,     AMAXW   =   17.0,
LFTAW   =   880.8, LFTDW   =  182.8,   LFTFW   =   263.3,
[Drag from ref. 9; (e=0.987)]:
DRG0W   =   9.244, DRGVW   =  0.0,     DRGIW   =  0.0003116,
DRGDW   =   10.68, DRGFW   =  4.40,
MOM0W   =  -119.2, MOMAW   =  1253.6,  MOMDW   =  -183.6, MOMFW   =  -263.5,
SIDEB   =  -83.1,  SIDEP   =  0.00,    SIDER   =   0.00,  SIDEA   =  0.00,
ROLLB   =   166.,  ROLLP   =  -75900., ROLLR   =   7900., ROLLA   =  -2901.,
YAWB    =  -1291., YAWP    =  -1700.,  YAWR    =  -1700., YAWA    =   48.6,
LFTAH   =   204.5, LFTEH   =   117.6,  AMAXH   =   15.0,  IHT     =  0.00,
LFTAV   =   153.0, LFTRV   =   59.1,   AMAXV   =   20.0,  IVT     =  0.00,
OPTINT  =      1,
```

```
FETAIL  =   2016., LHTAIL  =   22.0,   HVTAIL  =   2.75,
! Airframe/rotor aerodynamic interference (p. 156)
OPINTV  =   2*0,   OPI1BP  =   4*0,    OPI2BP  =   4*0,
NWING   =   0,     NBODY   =   0,
! Engine and drive train model (p. 159)
[IENG, KICS, and GSE revised per ref. 11]:
ENGPOS  = 3,          THRTLC = 18000.,        KEDAMP  = 1.07,
IENG    = 233.,       KMAST1 = 750000.,       KMAST2  = 750000.,
KICS    = 281000.,    KENG   = 1.49E+07,
GSE     = 0.01,       GSI    = 0.01,
KPGOVE  = 0.00,      KPGOV1  = 0.00,          KPGOV2  = 0.00,
KIGOVE  = 0.00,      KIGOV1  = 1.6666999E-02, KIGOV2  = 1.6666999E-02,
T1GOVE  = 0.222,     T1GOV1  = 0.222,         T1GOV2  =  0.222,
T2GOVE  = 2.54E-02, T2GOV1  = 2.54E-02,       T2GOV2  =  2.54E-02
$END
```

Airfoil Tables

For aerodynamic data input, each blade is divided into four radial segments: 0-0.2 *R*, 0.2-0.84 *R*, 0.84-0.95 *R*, and 0.95-1.0 *R*. (Different segments are used for computation; see RAE under NLRTR in the preceding namelist.) The airfoil sections used in each segment are, in order, Boeing V43030-1.58, VR-7 with –3° tab, a transition between VR-7 and VR-8, and VR-8 (with a 0.0078 increment in drag coefficient). Boeing supplied the airfoil data in C81 binary format for direct input into CAMRAD. The data are printed out below in four sets, in the same order as listed above, reorganized slightly for ease of reading and publication. The original comment fields are retained.

Close comparison of the notes in the tables with figure 3 reveals that the C81 radial segments do not exactly correspond with the true boundaries of the airfoils. Furthermore, the blade segments specified in the rotor namelist (RAE) do not include all of the blade cuff. So far as is known, the consequences are insignificant, but this remains unverified as of this writing.

C81 table for the first blade segment (0–0.2 *R*):

```
 921 523 V43030 T305 WITH DCD  543 839 2 9
        0.0000 0.2100 0.3000 0.4100 1.0000
-180.00 0.0053 0.0053 0.0053 0.0053 0.0053
 -90.00-0.0240-0.0240-0.0240-0.0240-0.0240
 -30.00-1.0615-1.0615-1.0615-1.0615-1.0615
 -20.00-1.0000-1.0000-1.0000-1.0000-1.0000
 -18.00-0.9360-0.9360-0.9480-0.9460-0.9460
 -16.00-0.8720-0.8720-0.8960-0.8920-0.8920
 -15.00-0.8400-0.8400-0.8700-0.8650-0.8650
 -14.00-0.8080-0.8080-0.8440-0.8380-0.8380
 -13.00-0.7760-0.7760-0.8180-0.8110-0.8110
 -12.00-0.7440-0.7440-0.7920-0.7840-0.7840
 -11.00-0.7120-0.7120-0.7660-0.7570-0.7570
 -10.00-0.6800-0.6800-0.7400-0.7300-0.7300
  -9.00-0.6600-0.6600-0.6850-0.6800-0.6800
  -8.00-0.5833-0.5833-0.6300-0.6300-0.6300
  -7.00-0.5067-0.5067-0.5400-0.5300-0.5300
  -6.00-0.4300-0.4300-0.4500-0.4300-0.4300
  -5.00-0.3267-0.3267-0.3433-0.3400-0.3400
  -4.00-0.2233-0.2233-0.2367-0.2500-0.2500
  -3.00-0.1200-0.1200-0.1300-0.1375-0.1375
  -2.00-0.0167-0.0167-0.0233-0.0250-0.0250
  -1.00 0.0867 0.0867 0.0833 0.0875 0.0875
   0.00 0.1900 0.1900 0.1900 0.2000 0.2000
   1.00 0.2962 0.2962 0.2975 0.3150 0.3150
   2.00 0.4025 0.4025 0.4050 0.4300 0.4300
   3.00 0.5087 0.5087 0.5125 0.5450 0.5450
   4.00 0.6150 0.6150 0.6200 0.6600 0.6600
   5.00 0.7212 0.7212 0.7275 0.7083 0.7083
   6.00 0.8275 0.8275 0.8350 0.7567 0.7567
   7.00 0.9337 0.9337 0.9425 0.8050 0.8050
   8.00 1.0400 1.0400 1.0500 0.8533 0.8533
   9.00 1.0729 1.0729 1.0714 0.9017 0.9017
  10.00 1.1057 1.1057 1.0929 0.9500 0.9500
  11.00 1.1386 1.1386 1.1143 0.9350 0.9350
  12.00 1.1714 1.1714 1.1357 0.9200 0.9200
  13.00 1.2043 1.2043 1.1571 0.9050 0.9050
  14.00 1.2371 1.2371 1.1786 0.8900 0.8900
  15.00 1.2700 1.2700 1.2000 0.8750 0.8750
  16.00 1.2400 1.2400 1.1800 0.8600 0.8600
  18.00 1.1800 1.1800 1.1400 0.8300 0.8300
  20.00 1.1200 1.1200 1.1000 0.8000 0.8000
```

30.00	1.0615	1.0615	1.0615	1.0615	1.0615			
90.00	0.0240	0.0240	0.0240	0.0240	0.0240			
180.00	0.0053	0.0053	0.0053	0.0053	0.0053			
	0.0000	0.3000	0.5000	0.6100	0.6500	0.7150	0.8500	1.0000
-180.00	0.0234	0.0234	0.0234	0.0234	0.0234	0.0234	0.0234	0.0234
-90.00	1.5574	1.5574	1.5574	1.5574	1.5574	1.5574	1.5574	1.5574
-30.00	0.7584	0.7584	0.7584	0.7584	0.7584	0.7584	0.7584	0.7584
-16.00	0.2975	0.3395	0.3675	0.3829	0.3885	0.3976	0.4165	0.4375
-15.00	0.2646	0.3096	0.3396	0.3561	0.3621	0.3719	0.3921	0.4146
-14.00	0.2317	0.2797	0.3117	0.3293	0.3357	0.3461	0.3677	0.3917
-13.00	0.1988	0.2498	0.2838	0.3025	0.3093	0.3203	0.3433	0.3688
-12.00	0.1658	0.2198	0.2558	0.2756	0.2828	0.2945	0.3188	0.3458
-11.00	0.1329	0.1899	0.2279	0.2488	0.2564	0.2688	0.2944	0.3229
-10.00	0.1000	0.1600	0.2000	0.2220	0.2300	0.2430	0.2700	0.3000
-9.00	0.0850	0.1300	0.1786	0.2053	0.2150	0.2308	0.2636	0.3000
-8.00	0.0700	0.1000	0.1571	0.1886	0.2000	0.2186	0.2571	0.3000
-7.00	0.0550	0.0700	0.1357	0.1719	0.1850	0.2064	0.2507	0.3000
-6.00	0.0400	0.0400	0.1143	0.1551	0.1700	0.1941	0.2443	0.3000
-5.00	0.0300	0.0300	0.0550	0.0687	0.0737	0.0910	0.1900	0.3000
-4.00	0.0230	0.0230	0.0410	0.0510	0.0546	0.0641	0.1759	0.3000
-3.00	0.0190	0.0190	0.0280	0.0406	0.0451	0.0563	0.1717	0.3000
-2.00	0.0150	0.0150	0.0150	0.0302	0.0357	0.0484	0.1676	0.3000
-1.00	0.0135	0.0135	0.0135	0.0276	0.0328	0.0450	0.1658	0.3000
0.00	0.0120	0.0120	0.0120	0.0251	0.0299	0.0415	0.1640	0.3000
1.00	0.0120	0.0120	0.0120	0.0293	0.0356	0.0494	0.1681	0.3000
2.00	0.0120	0.0120	0.0120	0.0335	0.0413	0.0573	0.1722	0.3000
3.00	0.0120	0.0120	0.0120	0.0453	0.0578	0.0804	0.1844	0.3000
4.00	0.0120	0.0120	0.0120	0.0571	0.0742	0.1034	0.1966	0.3000
5.00	0.0125	0.0125	0.0255	0.0552	0.0764	0.1116	0.2008	0.3000
6.00	0.0130	0.0130	0.0390	0.0533	0.0786	0.1197	0.2051	0.3000
7.00	0.0148	0.0148	0.0637	0.0907	0.1106	0.1428	0.2098	0.3000
8.00	0.0165	0.0165	0.0885	0.1281	0.1425	0.1659	0.2145	0.3000
9.00	0.0197	0.0197	0.0699	0.1164	0.1336	0.1616	0.2197	0.3000
10.00	0.0230	0.0230	0.0513	0.1046	0.1246	0.1572	0.2248	0.3000
11.00	0.0275	0.0275	0.0805	0.1285	0.1463	0.1749	0.2341	0.3000
12.00	0.0320	0.0320	0.1097	0.1525	0.1680	0.1925	0.2434	0.3000
13.00	0.0413	0.0413	0.1246	0.1638	0.1780	0.2007	0.2477	0.3000
14.00	0.0507	0.0507	0.1396	0.1752	0.1881	0.2089	0.2520	0.3000
15.00	0.0600	0.0600	0.1545	0.1865	0.1981	0.2171	0.2563	0.3000
16.00	0.1312	0.1312	0.1856	0.2182	0.2290	0.2467	0.2833	0.3241
30.00	0.6622	0.6622	0.6622	0.6622	0.6622	0.6622	0.6622	0.6622
90.00	1.5574	1.5574	1.5574	1.5574	1.5574	1.5574	1.5574	1.5574
180.00	0.0234	0.0234	0.0234	0.0234	0.0234	0.0234	0.0234	0.0234

```
        0.0000 1.0000
-180.00 0.0144 0.0144
 -90.00 0.5495 0.5495
 -30.00 0.1800 0.1800
 -16.00-0.0280-0.0280
   0.00-0.0280-0.0280
  16.00-0.0280-0.0280
  30.00-0.1773-0.1773
  90.00-0.5495-0.5495
 180.00 0.0144 0.0144

V43030-1.58
for Boeing advanced tilt rotor blade, r = 0-.2
from M. Sheffler, Boeing Vertol, January 1983
also ATB at OARF, from Randy Smith, Boeing Vertol, March 1984
```

C81 table for the second blade segment (0.2–0.84 *R*):

```
968 577/296  VR-7  -3 TAB     113911511047
        0.0000 0.2000 0.3000 0.4000 0.5000 0.6000 0.7000 0.7500 0.8000 0.9000 1.0000
-180.00 0.0053 0.0053 0.0053 0.0053 0.0053 0.0053 0.0053 0.0053 0.0053 0.0053 0.0053
-173.00 0.4863 0.4863 0.4863 0.4863 0.4863 0.4863 0.4863 0.4863 0.4863 0.4863 0.4863
-161.00 0.4896 0.4896 0.4896 0.4896 0.4896 0.4896 0.4896 0.4896 0.4896 0.4896 0.4896
-147.00 0.7929 0.7929 0.7929 0.7929 0.7929 0.7929 0.7929 0.7929 0.7929 0.7929 0.7929
-129.00 0.8406 0.8406 0.8406 0.8406 0.8406 0.8406 0.8406 0.8406 0.8406 0.8406 0.8406
 -49.00-1.0802-1.0802-1.0802-1.0802-1.0802-1.0802-1.0802-1.0802-1.0802-1.0802-1.0802
 -30.00-1.0615-1.0615-1.0615-1.0615-1.0615-1.0615-1.0615-1.0615-1.0615-1.0615-1.0615
 -20.00-0.8000-0.8000-0.8000-0.8000-0.8000-0.8000-0.8000-0.8000-0.8000-0.8000-0.8000
 -16.00-0.7200-0.7200-0.7200-0.7153-0.7147-0.7253-0.7229-0.7333-0.6895-0.6452-0.6452
 -12.00-0.6400-0.6400-0.6400-0.6307-0.6294-0.6507-0.6457-0.6666-0.5790-0.4903-0.4903
 -10.00-0.6000-0.6000-0.6000-0.5883-0.5867-0.6133-0.6072-0.6332-0.5237-0.4129-0.4129
  -8.00-0.5600-0.5600-0.5600-0.5460-0.5441-0.5760-0.5686-0.5999-0.4685-0.3355-0.3355
  -6.00-0.5200-0.5200-0.5200-0.5037-0.5014-0.5387-0.5300-0.5665-0.4132-0.2580-0.2580
  -5.00-0.4075-0.4075-0.4075-0.4021-0.4769-0.5200-0.5107-0.5499-0.3856-0.2193-0.2193
  -4.00-0.2950-0.2950-0.2950-0.3006-0.3484-0.3724-0.4193-0.5332-0.3580-0.1806-0.1806
  -3.00-0.1824-0.1824-0.1824-0.1990-0.2199-0.2249-0.2516-0.3278-0.3303-0.1419-0.1419
  -2.00-0.0699-0.0699-0.0699-0.0803-0.0907-0.0822-0.0839-0.1149-0.1958-0.1032-0.1032
  -1.00 0.0426 0.0426 0.0426 0.0384 0.0385 0.0604 0.0838 0.1019 0.0035-0.0645-0.0645
   0.00 0.1551 0.1551 0.1551 0.1571 0.1677 0.2030 0.2516 0.3132 0.1246 0.0483 0.0483
   1.00 0.2667 0.2667 0.2667 0.2752 0.2989 0.3479 0.4154 0.3664 0.2274 0.1765 0.1765
   2.00 0.3783 0.3783 0.3783 0.3932 0.4300 0.4927 0.5549 0.4574 0.2996 0.2199 0.2199
   3.00 0.4899 0.4899 0.4899 0.5112 0.5612 0.6376 0.6471 0.4875 0.3386 0.2632 0.2632
   4.00 0.6015 0.6015 0.6015 0.6292 0.6923 0.7824 0.7155 0.5177 0.3775 0.3065 0.3065
   5.00 0.7131 0.7131 0.7131 0.7472 0.8234 0.9273 0.7319 0.5478 0.4164 0.3499 0.3499
   6.00 0.8246 0.8246 0.8246 0.8652 0.9546 1.0583 0.7497 0.5780 0.4553 0.3932 0.3932
   7.00 0.9362 0.9362 0.9362 0.9832 1.0857 1.1137 0.7676 0.6081 0.4942 0.4366 0.4366
   8.00 1.0478 1.0478 1.0478 1.1013 1.2169 1.1694 0.7855 0.6383 0.5331 0.4799 0.4799
   9.00 1.1498 1.1498 1.1498 1.2191 1.3480 1.2251 0.8034 0.6684 0.5720 0.5232 0.5232
  10.00 1.2518 1.2518 1.2518 1.3182 1.4066 1.1946 0.8212 0.6986 0.6109 0.5666 0.5666
  12.00 1.4205 1.4205 1.4205 1.3351 1.4410 1.2027 0.8570 0.7588 0.6887 0.6533 0.6533
  16.00 1.1200 1.1200 1.1200 1.1115 1.2330 1.1013 0.9285 0.8794 0.8444 0.8266 0.8266
  20.00 1.0000 1.0000 1.0000 1.0000 1.0000 1.0000 1.0000 1.0000 1.0000 1.0000 1.0000
  30.00 1.0615 1.0615 1.0615 1.0615 1.0615 1.0615 1.0615 1.0615 1.0615 1.0615 1.0615
  49.00 1.0802 1.0802 1.0802 1.0802 1.0802 1.0802 1.0802 1.0802 1.0802 1.0802 1.0802
 129.00-0.8406-0.8406-0.8406-0.8406-0.8406-0.8406-0.8406-0.8406-0.8406-0.8406-0.8406
 147.00-0.7929-0.7929-0.7929-0.7929-0.7929-0.7929-0.7929-0.7929-0.7929-0.7929-0.7929
 161.00-0.4896-0.4896-0.4896-0.4896-0.4896-0.4896-0.4896-0.4896-0.4896-0.4896-0.4896
 173.00-0.4863-0.4863-0.4863-0.4863-0.4863-0.4863-0.4863-0.4863-0.4863-0.4863-0.4863
 180.00 0.0053 0.0053 0.0053 0.0053 0.0053 0.0053 0.0053 0.0053 0.0053 0.0053 0.0053
```

	0.0000	0.2000	0.3000	0.4000	0.5000	0.6000	0.7000	0.7500	0.8000	0.9000	1.0000
-180.00	0.0234	0.0234	0.0234	0.0234	0.0234	0.0234	0.0234	0.0234	0.0234	0.0234	0.0234
-175.00	0.0302	0.0302	0.0302	0.0302	0.0302	0.0302	0.0302	0.0302	0.0302	0.0302	0.0302
-170.00	0.0452	0.0452	0.0452	0.0452	0.0452	0.0452	0.0452	0.0452	0.0452	0.0452	0.0452
-165.00	0.0786	0.0786	0.0786	0.0786	0.0786	0.0786	0.0786	0.0786	0.0786	0.0786	0.0786
-160.00	0.3186	0.3186	0.3186	0.3186	0.3186	0.3186	0.3186	0.3186	0.3186	0.3186	0.3186
-140.00	0.8938	0.8938	0.8938	0.8938	0.8938	0.8938	0.8938	0.8938	0.8938	0.8938	0.8938
-120.00	1.2353	1.2353	1.2353	1.2353	1.2353	1.2353	1.2353	1.2353	1.2353	1.2353	1.2353
-110.00	1.3868	1.3868	1.3868	1.3868	1.3868	1.3868	1.3868	1.3868	1.3868	1.3868	1.3868
-100.00	1.5092	1.5092	1.5092	1.5092	1.5092	1.5092	1.5092	1.5092	1.5092	1.5092	1.5092
-90.00	1.5574	1.5574	1.5574	1.5574	1.5574	1.5574	1.5574	1.5574	1.5574	1.5574	1.5574
-80.00	1.5190	1.5190	1.5190	1.5190	1.5190	1.5190	1.5190	1.5190	1.5190	1.5190	1.5190
-70.00	1.4166	1.4166	1.4166	1.4166	1.4166	1.4166	1.4166	1.4166	1.4166	1.4166	1.4166
-60.00	1.2855	1.2855	1.2855	1.2855	1.2855	1.2855	1.2855	1.2855	1.2855	1.2855	1.2855
-50.00	1.1439	1.1439	1.1439	1.1439	1.1439	1.1439	1.1439	1.1439	1.1439	1.1439	1.1439
-40.00	0.9937	0.9937	0.9937	0.9937	0.9937	0.9937	0.9937	0.9937	0.9937	0.9937	0.9937
-30.00	0.8196	0.8196	0.8196	0.8196	0.8196	0.8196	0.8196	0.8196	0.8196	0.8196	0.8196
-6.00	0.0087	0.0087	0.0087	0.0261	0.0427	0.0593	0.0759	0.0842	0.1138	0.1778	0.2418
-5.00	0.0085	0.0085	0.0085	0.0173	0.0266	0.0397	0.0568	0.0663	0.0971	0.1611	0.2251
-4.00	0.0085	0.0085	0.0085	0.0085	0.0104	0.0201	0.0378	0.0485	0.0805	0.1445	0.2085
-3.00	0.0085	0.0085	0.0085	0.0085	0.0087	0.0094	0.0160	0.0267	0.0587	0.1227	0.1867
-2.00	0.0085	0.0085	0.0085	0.0085	0.0085	0.0086	0.0120	0.0240	0.0560	0.1200	0.1840
-1.00	0.0085	0.0085	0.0085	0.0085	0.0085	0.0085	0.0100	0.0233	0.0553	0.1193	0.1833
0.00	0.0085	0.0085	0.0085	0.0085	0.0085	0.0085	0.0124	0.0380	0.0700	0.1340	0.1980
1.00	0.0085	0.0085	0.0085	0.0085	0.0085	0.0085	0.0205	0.0530	0.0856	0.1507	0.2158
2.00	0.0085	0.0085	0.0085	0.0085	0.0085	0.0085	0.0376	0.0696	0.1016	0.1656	0.2296
3.00	0.0085	0.0085	0.0085	0.0085	0.0085	0.0088	0.0504	0.0824	0.1144	0.1784	0.2424
4.00	0.0085	0.0085	0.0085	0.0088	0.0089	0.0096	0.0632	0.0952	0.1272	0.1912	0.2552
5.00	0.0087	0.0087	0.0087	0.0093	0.0100	0.0118	0.0758	0.1078	0.1398	0.2038	0.2678
6.00	0.0088	0.0088	0.0088	0.0099	0.0101	0.0310	0.0950	0.1270	0.1590	0.2230	0.2870
7.00	0.0093	0.0093	0.0093	0.0101	0.0109	0.0489	0.1129	0.1449	0.1769	0.2409	0.3049
8.00	0.0098	0.0098	0.0098	0.0119	0.0148	0.0650	0.1290	0.1610	0.1930	0.2570	0.3210
9.00	0.0125	0.0125	0.0125	0.0131	0.0144	0.0784	0.1424	0.1744	0.2064	0.2704	0.3344
10.00	0.0150	0.0150	0.0150	0.0150	0.0348	0.0988	0.1628	0.1948	0.2268	0.2908	0.3548
11.00	0.0170	0.0170	0.0170	0.0174	0.0814	0.1454	0.2094	0.2414	0.2734	0.3374	0.4014
12.00	0.0194	0.0194	0.0194	0.0815	0.1455	0.2095	0.2735	0.3055	0.3375	0.4015	0.4655
13.00	0.0500	0.0500	0.0500	0.1143	0.1786	0.2429	0.3071	0.3393	0.3714	0.4357	0.5000
30.00	0.7039	0.7039	0.7039	0.7039	0.7039	0.7039	0.7039	0.7039	0.7039	0.7039	0.7039
50.00	1.0907	1.0907	1.0907	1.0907	1.0907	1.0907	1.0907	1.0907	1.0907	1.0907	1.0907
60.00	1.2475	1.2475	1.2475	1.2475	1.2475	1.2475	1.2475	1.2475	1.2475	1.2475	1.2475
70.00	1.3941	1.3941	1.3941	1.3941	1.3941	1.3941	1.3941	1.3941	1.3941	1.3941	1.3941
80.00	1.5117	1.5117	1.5117	1.5117	1.5117	1.5117	1.5117	1.5117	1.5117	1.5117	1.5117
90.00	1.5574	1.5574	1.5574	1.5574	1.5574	1.5574	1.5574	1.5574	1.5574	1.5574	1.5574
100.00	1.5092	1.5092	1.5092	1.5092	1.5092	1.5092	1.5092	1.5092	1.5092	1.5092	1.5092

110.00	1.3868	1.3868	1.3868	1.3868	1.3868	1.3868	1.3868	1.3868	1.3868	1.3868	1.3868
120.00	1.2353	1.2353	1.2353	1.2353	1.2353	1.2353	1.2353	1.2353	1.2353	1.2353	1.2353
140.00	0.8938	0.8938	0.8938	0.8938	0.8938	0.8938	0.8938	0.8938	0.8938	0.8938	0.8938
160.00	0.3186	0.3186	0.3186	0.3186	0.3186	0.3186	0.3186	0.3186	0.3186	0.3186	0.3186
165.00	0.0786	0.0786	0.0786	0.0786	0.0786	0.0786	0.0786	0.0786	0.0786	0.0786	0.0786
170.00	0.0452	0.0452	0.0452	0.0452	0.0452	0.0452	0.0452	0.0452	0.0452	0.0452	0.0452
175.00	0.0302	0.0302	0.0302	0.0302	0.0302	0.0302	0.0302	0.0302	0.0302	0.0302	0.0302
180.00	0.0234	0.0234	0.0234	0.0234	0.0234	0.0234	0.0234	0.0234	0.0234	0.0234	0.0234
	0.0000	0.3000	0.4000	0.5000	0.6000	0.6500	0.7000	0.7500	0.8000	1.0000	
-180.00	0.0144	0.0144	0.0144	0.0144	0.0144	0.0144	0.0144	0.0144	0.0144	0.0144	
-170.00	0.3270	0.3270	0.3270	0.3270	0.3270	0.3270	0.3270	0.3270	0.3270	0.3270	
-165.00	0.2939	0.2939	0.2939	0.2939	0.2939	0.2939	0.2939	0.2939	0.2939	0.2939	
-160.00	0.3098	0.3098	0.3098	0.3098	0.3098	0.3098	0.3098	0.3098	0.3098	0.3098	
-135.00	0.5548	0.5548	0.5548	0.5548	0.5548	0.5548	0.5548	0.5548	0.5548	0.5548	
-90.00	0.5495	0.5495	0.5495	0.5495	0.5495	0.5495	0.5495	0.5495	0.5495	0.5495	
-30.00	0.1800	0.1800	0.1800	0.1800	0.1800	0.1800	0.1800	0.1800	0.1800	0.1800	
-20.00	0.1522	0.1522	0.1522	0.1522	0.1522	0.1522	0.1522	0.1522	0.1522	0.1522	
-16.00	0.1400	0.1400	0.1400	0.1400	0.1400	0.1400	0.1400	0.1400	0.1400	0.1400	
-15.00	0.1352	0.1352	0.1352	0.1352	0.1352	0.1352	0.1352	0.1352	0.1352	0.1352	
-14.00	0.1294	0.1294	0.1294	0.1294	0.1294	0.1294	0.1294	0.1294	0.1294	0.1294	
-13.00	0.0974	0.0974	0.0962	0.0962	0.0964	0.0982	0.1000	0.1011	0.1016	0.1100	
-12.00	0.0832	0.0832	0.0816	0.0816	0.0819	0.0843	0.0867	0.0881	0.0888	0.1000	
-11.00	0.0690	0.0690	0.0670	0.0670	0.0674	0.0704	0.0733	0.0752	0.0760	0.0900	
-10.00	0.0548	0.0548	0.0524	0.0524	0.0529	0.0564	0.0600	0.0622	0.0632	0.0800	
-9.00	0.0406	0.0406	0.0378	0.0378	0.0384	0.0425	0.0467	0.0492	0.0504	0.0700	
-8.00	0.0264	0.0264	0.0232	0.0232	0.0239	0.0286	0.0333	0.0363	0.0376	0.0600	
-7.00	0.0122	0.0122	0.0086	0.0086	0.0093	0.0146	0.0200	0.0233	0.0248	0.0500	
-6.00	-0.0020	-0.0020	-0.0060	-0.0060	-0.0052	0.0007	0.0067	0.0103	0.0120	0.0400	
-4.00	-0.0010	-0.0010	-0.0030	-0.0070	-0.0135	-0.0180	-0.0220	-0.0253	-0.0320	0.0020	
-3.00	-0.0035	-0.0035	-0.0045	-0.0075	-0.0122	-0.0159	-0.0203	-0.0268	-0.0410	-0.0300	
-2.00	-0.0060	-0.0060	-0.0060	-0.0080	-0.0108	-0.0139	-0.0187	-0.0283	-0.0500	-0.0620	
-1.00	-0.0075	-0.0075	-0.0080	-0.0100	-0.0128	-0.0153	-0.0220	-0.0398	-0.0790	-0.0770	
0.00	-0.0090	-0.0090	-0.0100	-0.0120	-0.0148	-0.0167	-0.0253	-0.0513	-0.1080	-0.0920	
1.00	-0.0110	-0.0110	-0.0120	-0.0150	-0.0180	-0.0197	-0.0347	-0.0698	-0.1090	-0.1510	
2.00	-0.0140	-0.0140	-0.0150	-0.0175	-0.0208	-0.0244	-0.0430	-0.0812	-0.1120	-0.1860	
3.00	-0.0170	-0.0170	-0.0180	-0.0210	-0.0238	-0.0303	-0.0507	-0.0883	-0.1200	-0.2360	
4.00	-0.0200	-0.0200	-0.0220	-0.0230	-0.0263	-0.0428	-0.0663	-0.0955	-0.1280	-0.2700	
6.00	-0.0280	-0.0280	-0.0270	-0.0280	-0.0282	-0.0560	-0.0847	-0.1080	-0.1480	-0.3100	
7.00	-0.0320	-0.0320	-0.0300	-0.0300	-0.0332	-0.0637	-0.0937	-0.1172	-0.1580	-0.3200	
8.00	-0.0350	-0.0350	-0.0320	-0.0320	-0.0470	-0.0744	-0.0993	-0.1233	-0.1700	-0.3500	
9.00	-0.0370	-0.0370	-0.0335	-0.0305	-0.0553	-0.0826	-0.1058	-0.1304	-0.1800	-0.3500	
10.00	-0.0390	-0.0390	-0.0350	-0.0290	-0.0637	-0.0909	-0.1123	-0.1375	-0.1900	-0.3500	
11.00	-0.0405	-0.0405	-0.0355	-0.0230	-0.0706	-0.0963	-0.1177	-0.1442	-0.2000	-0.3500	
12.00	-0.0420	-0.0420	-0.0360	-0.0170	-0.0775	-0.1017	-0.1230	-0.1508	-0.2100	-0.3500	

```
  13.00-0.0450-0.0450-0.0580-0.0450-0.0877-0.1086-0.1290-0.1575-0.2200-0.3500
  14.00-0.0516-0.0516-0.0644-0.0516-0.0937-0.1143-0.1345-0.1626-0.2243-0.3526
  15.00-0.0581-0.0581-0.0708-0.0581-0.0997-0.1201-0.1399-0.1677-0.2286-0.3552
  16.00-0.0647-0.0647-0.0771-0.0647-0.1057-0.1258-0.1454-0.1728-0.2328-0.3578
  20.00-0.0909-0.0909-0.1027-0.0909-0.1297-0.1487-0.1672-0.1931-0.2500-0.3681
  30.00-0.1564-0.1564-0.1665-0.1564-0.1897-0.2059-0.2218-0.2440-0.2927-0.3940
  90.00-0.5495-0.5495-0.5495-0.5495-0.5495-0.5495-0.5495-0.5495-0.5495-0.5495
 135.00-0.5548-0.5548-0.5548-0.5548-0.5548-0.5548-0.5548-0.5548-0.5548-0.5548
 160.00-0.3098-0.3098-0.3098-0.3098-0.3098-0.3098-0.3098-0.3098-0.3098-0.3098
 165.00-0.2939-0.2939-0.2939-0.2939-0.2939-0.2939-0.2939-0.2939-0.2939-0.2939
 170.00-0.3270-0.3270-0.3270-0.3270-0.3270-0.3270-0.3270-0.3270-0.3270-0.3270
 180.00 0.0144 0.0144 0.0144 0.0144 0.0144 0.0144 0.0144 0.0144 0.0144 0.0144

VR7, Tab=3
for Boeing Advanced Tilt Rotor Blade, R = .2-.84
replaces airfoil deck 925/VR7T3D1, lower drag
from Randy Smith, Boeing Vertol, May 1985
```

C81 table for the third blade segment (0.84–0.95 *R*):

```
 923 284 VR-8 0 TAB DCD=.001  133420391437
        0.0000 0.3020 0.4010 0.5040 0.5600 0.5870 0.6170 0.6630 0.7130 0.7600 0.8200 0.9000 1.0000
-180.00 0.0053 0.0053 0.0053 0.0053 0.0053 0.0053 0.0053 0.0053 0.0053 0.0053 0.0053 0.0053 0.0053
 -30.00-1.0615-1.0615-1.0615-1.0615-1.0615-1.0615-1.0615-1.0615-1.0615-1.0615-1.0615-1.0615-1.0615
 -16.00-0.9868-0.9260-0.9352-0.9342-0.9360-0.9384-0.9302-0.9302-0.9648-0.9784-1.2975-1.6200-1.4800
 -14.00-0.9802-0.8890-0.9028-0.9014-0.9040-0.9076-0.8953-0.8953-0.9472-0.9676-1.1962-1.4300-1.2950
 -13.00-0.9769-0.8705-0.8866-0.8849-0.8880-0.8922-0.8779-0.8779-0.9384-0.9622-1.1456-1.3350-1.2025
 -12.00-0.9736-0.8520-0.8704-0.8685-0.8720-0.8768-0.8604-0.8604-0.9296-0.9568-1.0950-1.2400-1.1100
 -11.00-0.9703-0.8335-0.8542-0.8520-0.8560-0.8614-0.8430-0.8430-0.9208-0.9514-1.0444-1.1450-1.0175
 -10.00-0.9670-0.8150-0.8380-0.8356-0.8400-0.8460-0.8255-0.8255-0.9120-0.9460-0.9938-1.0500-0.9250
  -9.00-0.8609-0.7595-0.7840-0.7923-0.7867-0.7973-0.8062-0.8116-0.9071-0.9485-0.9431-0.9550-0.8325
  -8.00-0.7548-0.7040-0.7300-0.7490-0.7333-0.7487-0.7870-0.7978-0.9022-0.9510-0.8925-0.8600-0.7400
  -7.00-0.6487-0.6225-0.6460-0.6625-0.6800-0.7000-0.7018-0.7497-0.8501-0.8941-0.8419-0.7650-0.6475
  -6.00-0.5426-0.5410-0.5620-0.5760-0.5800-0.5963-0.6165-0.7016-0.7980-0.8373-0.7913-0.6700-0.5550
  -5.00-0.4365-0.4390-0.4615-0.4795-0.4800-0.4927-0.5183-0.5683-0.6432-0.6998-0.7406-0.5500-0.4625
  -4.00-0.3304-0.3370-0.3610-0.3830-0.3800-0.3890-0.4200-0.4350-0.4884-0.5623-0.6900-0.4300-0.3700
  -3.00-0.2243-0.2290-0.2464-0.2598-0.2575-0.2625-0.2848-0.2963-0.3338-0.3867-0.4812-0.3038-0.2775
  -2.00-0.1182-0.1210-0.1317-0.1365-0.1350-0.1360-0.1495-0.1575-0.1792-0.2112-0.2725-0.1775-0.1850
  -1.00-0.0121-0.0130-0.0171-0.0132-0.0125-0.0095-0.0143-0.0188-0.0246-0.0356-0.0038-0.0513-0.0925
   0.00 0.0940 0.0950 0.0975 0.1100 0.1100 0.1170 0.1210 0.1200 0.1300 0.1400 0.2650 0.0750-0.0000
   1.00 0.2004 0.2031 0.2100 0.2300 0.2357 0.2460 0.2544 0.2646 0.2871 0.3233 0.4700 0.2017 0.0925
   2.00 0.3067 0.3112 0.3225 0.3500 0.3614 0.3750 0.3879 0.4092 0.4442 0.5067 0.5700 0.3283 0.1850
   4.00 0.5195 0.5275 0.5475 0.5900 0.6129 0.6330 0.6547 0.6985 0.7585 0.7830 0.7167 0.6340 0.3700
   5.00 0.6258 0.6356 0.6600 0.7100 0.7386 0.7620 0.7881 0.8431 0.9031 0.8203 0.7900 0.8130 0.4625
   6.00 0.7322 0.7437 0.7725 0.8300 0.8643 0.8910 0.9216 0.9877 0.9525 0.8576 0.9007 0.9920 0.5550
   7.00 0.8385 0.8519 0.8850 0.9500 0.9900 1.0200 1.0550 1.0924 0.9961 0.8950 1.0113 1.1710 0.6475
   8.00 0.9449 0.9600 0.9590 1.0167 1.0900 1.1200 1.1620 1.1571 1.0830 0.9323 1.1220 1.3500 0.7400
   9.00 1.0300 1.0200 1.0100 1.0500 1.1500 1.1755 1.2400 1.2045 1.1700 1.0397 1.2327 1.4417 0.8325
  10.00 1.0300 1.0400 1.0225 1.0500 1.1000 1.1623 1.1467 1.1500 1.2233 1.1471 1.3433 1.5333 0.9250
  11.00 1.0300 1.0600 1.0350 1.0500 1.0840 1.1162 1.1300 1.1600 1.2480 1.2545 1.4540 1.6250 1.0175
  12.00 1.0300 1.0659 1.0475 1.0560 1.0680 1.0700 1.1133 1.1700 1.2440 1.3618 1.5647 1.7167 1.1100
  13.00 1.0300 1.0718 1.0612 1.0680 1.0643 1.0725 1.0967 1.1800 1.2400 1.4692 1.6753 1.8083 1.2025
  14.00 1.0300 1.0776 1.0750 1.0800 1.0729 1.0750 1.0800 1.1900 1.2867 1.5766 1.7860 1.9000 1.2950
  16.00 1.0300 1.0429 1.0333 1.0633 1.0900 1.0800 1.1067 1.2100 1.3800 1.8372 2.0073 2.0833 1.4800
  30.00 1.0615 1.0615 1.0615 1.0615 1.0615 1.0615 1.0615 1.0615 1.0615 1.0615 1.0615 1.0615 1.0615
 180.00 0.0053 0.0053 0.0053 0.0053 0.0053 0.0053 0.0053 0.0053 0.0053 0.0053 0.0053 0.0053 0.0053
```

	0.0000	0.2000	0.2500	0.3000	0.4000	0.5000	0.5580	0.5820	0.6000	0.6480
	0.6750	0.7100	0.7500	0.7750	0.8200	0.8400	0.8750	0.8900	0.9000	1.0000
-180.00	0.0244	0.0244	0.0244	0.0244	0.0244	0.0244	0.0244	0.0244	0.0244	0.0244
	0.0244	0.0244	0.0244	0.0244	0.0244	0.0244	0.0244	0.0244	0.0244	0.0244
-90.00	1.5584	1.5584	1.5584	1.5584	1.5584	1.5584	1.5584	1.5584	1.5584	1.5584
	1.5584	1.5584	1.5584	1.5584	1.5584	1.5584	1.5584	1.5584	1.5584	1.5584
-30.00	0.8206	0.8206	0.8206	0.8206	0.8206	0.8206	0.8206	0.8206	0.8206	0.8206
	0.8206	0.8206	0.8206	0.8206	0.8206	0.8206	0.8206	0.8206	0.8206	0.8206
-16.00	0.4729	0.4729	0.4729	0.4729	0.4729	0.4729	0.4729	0.4729	0.4729	0.4729
	0.4729	0.4729	0.4729	0.4729	0.4729	0.4729	0.4729	0.4729	0.4729	0.4729
-15.00	0.4404	0.4404	0.4404	0.4404	0.4404	0.4404	0.4404	0.4404	0.4404	0.4404
	0.4404	0.4404	0.4404	0.4404	0.4404	0.4404	0.4404	0.4404	0.4404	0.4404
-14.00	0.4066	0.4066	0.4066	0.4066	0.4066	0.4066	0.4066	0.4066	0.4066	0.4066
	0.4066	0.4066	0.4066	0.4066	0.4066	0.4066	0.4066	0.4066	0.4066	0.4066
-13.00	0.3714	0.3714	0.3714	0.3714	0.3714	0.3714	0.3714	0.3714	0.3714	0.3714
	0.3714	0.3714	0.3714	0.3714	0.3714	0.3714	0.3714	0.3714	0.3714	0.3714
-12.00	0.3347	0.3347	0.3347	0.3347	0.3347	0.3347	0.3347	0.3347	0.3347	0.3347
	0.3347	0.3347	0.3347	0.3347	0.3347	0.3347	0.3347	0.3347	0.3347	0.3347
-11.00	0.2965	0.2965	0.2965	0.2965	0.2965	0.2965	0.2965	0.2965	0.2965	0.2965
	0.2965	0.2965	0.2965	0.2965	0.2965	0.2965	0.2965	0.2965	0.2965	0.2965
-10.00	0.2431	0.2442	0.2445	0.2448	0.2454	0.2459	0.2472	0.2477	0.2475	0.2493
	0.2509	0.2529	0.2571	0.2603	0.2662	0.2688	0.2733	0.2753	0.2766	0.2896
-9.00	0.1898	0.1920	0.1925	0.1931	0.1942	0.1953	0.1978	0.1989	0.1986	0.2021
	0.2053	0.2093	0.2176	0.2241	0.2358	0.2411	0.2501	0.2541	0.2567	0.2827
-8.00	0.1364	0.1397	0.1406	0.1414	0.1431	0.1448	0.1485	0.1501	0.1496	0.1550
	0.1597	0.1658	0.1782	0.1879	0.2055	0.2133	0.2270	0.2328	0.2367	0.2758
-7.00	0.0831	0.0875	0.0886	0.0897	0.0919	0.0942	0.0991	0.1013	0.1007	0.1078
	0.1141	0.1222	0.1387	0.1517	0.1751	0.1856	0.2038	0.2116	0.2168	0.2689
-6.00	0.0297	0.0352	0.0366	0.0380	0.0408	0.0436	0.0498	0.0525	0.0517	0.0606
	0.0685	0.0786	0.0993	0.1155	0.1448	0.1579	0.1806	0.1904	0.1969	0.2620
-5.00	0.0203	0.0231	0.0238	0.0249	0.0272	0.0295	0.0331	0.0346	0.0344	0.0392
	0.0450	0.0541	0.0690	0.0827	0.1105	0.1208	0.1378	0.1451	0.1500	0.1825
-4.00	0.0110	0.0110	0.0110	0.0119	0.0136	0.0154	0.0164	0.0167	0.0170	0.0178
	0.0214	0.0295	0.0387	0.0498	0.0761	0.0838	0.0950	0.0998	0.1030	0.1030
-3.00	0.0098	0.0098	0.0098	0.0103	0.0112	0.0121	0.0125	0.0127	0.0129	0.0131
	0.0148	0.0189	0.0239	0.0296	0.0453	0.0524	0.0749	0.0846	0.0910	0.0910
-2.00	0.0087	0.0087	0.0087	0.0087	0.0087	0.0087	0.0087	0.0087	0.0087	0.0084
	0.0082	0.0083	0.0090	0.0095	0.0146	0.0210	0.0548	0.0693	0.0790	0.0790
-1.00	0.0088	0.0087	0.0086	0.0086	0.0085	0.0084	0.0084	0.0084	0.0084	0.0083
	0.0083	0.0083	0.0089	0.0092	0.0154	0.0313	0.0612	0.0740	0.0740	0.0740
0.00	0.0088	0.0085	0.0084	0.0083	0.0082	0.0080	0.0081	0.0082	0.0082	0.0084
	0.0084	0.0085	0.0097	0.0115	0.0252	0.0395	0.0645	0.0658	0.0666	0.0750

1.00	0.0080	0.0076	0.0076	0.0075	0.0073	0.0076	0.0078	0.0078	0.0079	0.0080
	0.0081	0.0082	0.0094	0.0165	0.0410	0.0507	0.0678	0.0751	0.0775	0.0775
2.00	0.0080	0.0078	0.0077	0.0076	0.0075	0.0077	0.0077	0.0077	0.0077	0.0079
	0.0081	0.0083	0.0121	0.0244	0.0545	0.0616	0.0740	0.0793	0.0829	0.0850
3.00	0.0085	0.0083	0.0083	0.0082	0.0081	0.0080	0.0080	0.0079	0.0079	0.0084
	0.0088	0.0102	0.0254	0.0411	0.0665	0.0734	0.0856	0.0908	0.0943	0.0960
4.00	0.0085	0.0083	0.0082	0.0081	0.0080	0.0082	0.0083	0.0084	0.0084	0.0085
	0.0106	0.0202	0.0508	0.0642	0.0811	0.0886	0.1017	0.1073	0.1110	0.1210
5.00	0.0087	0.0086	0.0086	0.0086	0.0085	0.0088	0.0090	0.0101	0.0108	0.0205
	0.0299	0.0456	0.0685	0.0799	0.0969	0.1044	0.1176	0.1233	0.1270	0.1510
6.00	0.0090	0.0090	0.0090	0.0090	0.0090	0.0094	0.0097	0.0118	0.0133	0.0324
	0.0492	0.0710	0.0862	0.0957	0.1127	0.1203	0.1336	0.1393	0.1431	0.1810
7.00	0.0125	0.0110	0.0119	0.0129	0.0148	0.0157	0.0204	0.0246	0.0278	0.0507
	0.0676	0.0895	0.1097	0.1224	0.1451	0.1552	0.1729	0.1804	0.1855	0.2360
8.00	0.0160	0.0130	0.0149	0.0168	0.0206	0.0219	0.0311	0.0375	0.0423	0.0690
	0.0860	0.1081	0.1333	0.1491	0.1775	0.1901	0.2122	0.2216	0.2279	0.2910
9.00	0.0298	0.0358	0.0387	0.0415	0.0472	0.0516	0.0702	0.0792	0.0860	0.1068
	0.1226	0.1467	0.1660	0.1806	0.2087	0.2212	0.2430	0.2524	0.2586	0.3210
10.00	0.0435	0.0587	0.0624	0.0662	0.0738	0.0814	0.1094	0.1209	0.1296	0.1446
	0.1592	0.1853	0.1987	0.2121	0.2399	0.2522	0.2738	0.2831	0.2893	0.3510
11.00	0.0697	0.0953	0.1017	0.1081	0.1209	0.1322	0.1505	0.1581	0.1638	0.1804
	0.1928	0.2150	0.2393	0.2548	0.2830	0.2956	0.3176	0.3270	0.3332	0.3960
12.00	0.0960	0.1320	0.1410	0.1500	0.1680	0.1830	0.1917	0.1953	0.1980	0.2162
	0.2265	0.2448	0.2799	0.2975	0.3262	0.3389	0.3613	0.3708	0.3772	0.4410
13.00	0.1293	0.1693	0.1793	0.1893	0.2040	0.2160	0.2230	0.2258	0.2280	0.2574
	0.2739	0.2987	0.3364	0.3500	0.3691	0.3776	0.3925	0.3989	0.4031	0.4457
14.00	0.1627	0.2067	0.2177	0.2287	0.2400	0.2490	0.2542	0.2564	0.2580	0.2986
	0.3214	0.3526	0.3930	0.4025	0.4121	0.4163	0.4238	0.4269	0.4291	0.4503
15.00	0.1960	0.2440	0.2560	0.2680	0.2760	0.2820	0.2855	0.2869	0.2880	0.3397
	0.3688	0.4065	0.4496	0.4550	0.4550	0.4550	0.4550	0.4550	0.4550	0.4550
16.00	0.2271	0.2719	0.2831	0.2943	0.3018	0.3074	0.3107	0.3120	0.3130	0.3613
	0.3884	0.4236	0.4638	0.4689	0.4689	0.4689	0.4689	0.4689	0.4689	0.4689
30.00	0.6632	0.6632	0.6632	0.6632	0.6632	0.6632	0.6632	0.6632	0.6632	0.6632
	0.6632	0.6632	0.6632	0.6632	0.6632	0.6632	0.6632	0.6632	0.6632	0.6632
90.00	1.5584	1.5584	1.5584	1.5584	1.5584	1.5584	1.5584	1.5584	1.5584	1.5584
	1.5584	1.5584	1.5584	1.5584	1.5584	1.5584	1.5584	1.5584	1.5584	1.5584
180.00	0.0244	0.0244	0.0244	0.0244	0.0244	0.0244	0.0244	0.0244	0.0244	0.0244
	0.0244	0.0244	0.0244	0.0244	0.0244	0.0244	0.0244	0.0244	0.0244	0.0244

	0.0000	0.3000	0.4000	0.4570	0.5000	0.5600	0.5800	0.6100	0.6600	0.7100	0.7600	0.8500	0.9000	1.0000
-180.00	0.0144	0.0144	0.0144	0.0144	0.0144	0.0144	0.0144	0.0144	0.0144	0.0144	0.0144	0.0144	0.0144	0.0144
-30.00	0.1800	0.1800	0.1800	0.1800	0.1800	0.1800	0.1800	0.1800	0.1800	0.1800	0.1800	0.1800	0.1800	0.1800
-16.00	0.0946	0.0946	0.0946	0.0987	0.1018	0.1061	0.1076	0.1097	0.1133	0.1169	0.1205	0.1743	0.2042	0.2640
-15.00	0.0885	0.0885	0.0885	0.0929	0.0962	0.1008	0.1024	0.1047	0.1085	0.1124	0.1163	0.1739	0.2060	0.2700
-14.00	0.0824	0.0824	0.0824	0.0871	0.0906	0.0955	0.0972	0.0997	0.1038	0.1079	0.1120	0.1735	0.2077	0.2760
-13.00	0.0763	0.0763	0.0763	0.0813	0.0851	0.0902	0.0920	0.0947	0.0990	0.1034	0.1078	0.1731	0.2094	0.2820
-12.00	0.0702	0.0702	0.0702	0.0755	0.0795	0.0850	0.0869	0.0896	0.0942	0.0989	0.1035	0.1727	0.2111	0.2880
-11.00	0.0641	0.0641	0.0641	0.0697	0.0739	0.0797	0.0817	0.0846	0.0895	0.0944	0.0993	0.1723	0.2129	0.2940
-10.00	0.0580	0.0580	0.0580	0.0639	0.0683	0.0744	0.0765	0.0796	0.0847	0.0899	0.0950	0.1719	0.2146	0.3000
-9.00	0.0290	0.0320	0.0329	0.0364	0.0423	0.0505	0.0532	0.0573	0.0641	0.0709	0.0923	0.1646	0.2047	0.2850
-8.00	-0.0000	0.0059	0.0079	0.0090	0.0163	0.0265	0.0299	0.0350	0.0435	0.0520	0.0896	0.1572	0.1948	0.2700
-7.00	-0.0050	-0.0020	-0.0011	-0.0005	0.0032	0.0083	0.0100	0.0125	0.0126	0.0201	0.0592	0.1296	0.1774	0.1850
-6.00	-0.0100	-0.0100	-0.0100	-0.0100	-0.0100	-0.0100	-0.0100	-0.0100	-0.0182	-0.0118	0.0288	0.1019	0.1600	0.1000
-5.00	-0.0100	-0.0100	-0.0100	-0.0100	-0.0100	-0.0103	-0.0110	-0.0119	-0.0176	-0.0145	0.0057	0.0422	0.0711	0.0410
-4.00	-0.0100	-0.0100	-0.0100	-0.0100	-0.0100	-0.0106	-0.0119	-0.0138	-0.0170	-0.0171	-0.0173	-0.0176	-0.0177	-0.0180
-3.00	-0.0137	-0.0113	-0.0105	-0.0105	-0.0105	-0.0108	-0.0115	-0.0124	-0.0141	-0.0142	-0.0143	-0.0146	-0.0147	-0.0150
-2.00	-0.0174	-0.0126	-0.0110	-0.0110	-0.0110	-0.0110	-0.0110	-0.0110	-0.0111	-0.0113	-0.0114	-0.0116	-0.0117	-0.0120
-1.00	-0.0155	-0.0134	-0.0127	-0.0127	-0.0128	-0.0128	-0.0129	-0.0129	-0.0130	-0.0131	-0.0132	-0.0133	-0.0134	-0.0135
0.00	-0.0135	-0.0141	-0.0143	-0.0145	-0.0146	-0.0147	-0.0147	-0.0148	-0.0149	-0.0150	-0.0151	-0.0153	-0.0154	-0.0156
1.00	-0.0151	-0.0158	-0.0160	-0.0162	-0.0163	-0.0164	-0.0165	-0.0165	-0.0166	-0.0167	-0.0169	-0.0171	-0.0172	-0.0174
2.00	-0.0168	-0.0175	-0.0178	-0.0179	-0.0180	-0.0181	-0.0182	-0.0183	-0.0184	-0.0185	-0.0186	-0.0188	-0.0190	-0.0192
3.00	-0.0179	-0.0185	-0.0187	-0.0188	-0.0189	-0.0190	-0.0191	-0.0191	-0.0192	-0.0193	-0.0194	-0.0196	-0.0197	-0.0199
4.00	-0.0190	-0.0195	-0.0196	-0.0197	-0.0198	-0.0199	-0.0199	-0.0200	-0.0201	-0.0201	-0.0202	-0.0204	-0.0204	-0.0206
5.00	-0.0210	-0.0203	-0.0201	-0.0199	-0.0198	-0.0197	-0.0197	-0.0197	-0.0198	-0.0198	-0.0199	-0.0199	-0.0200	-0.0200
6.00	-0.0230	-0.0211	-0.0205	-0.0201	-0.0199	-0.0195	-0.0195	-0.0195	-0.0195	-0.0195	-0.0195	-0.0195	-0.0195	-0.0195
7.00	-0.0262	-0.0214	-0.0198	-0.0189	-0.0185	-0.0185	-0.0185	-0.0186	-0.0188	-0.0189	-0.0191	-0.0193	-0.0195	-0.0197
8.00	-0.0295	-0.0218	-0.0192	-0.0177	-0.0171	-0.0174	-0.0176	-0.0177	-0.0180	-0.0183	-0.0186	-0.0191	-0.0194	-0.0200
9.00	-0.0295	-0.0229	-0.0222	-0.0246	-0.0267	-0.0303	-0.0315	-0.0333	-0.0363	-0.0392	-0.0422	-0.0476	-0.0505	-0.0565
10.00	-0.0295	-0.0240	-0.0251	-0.0316	-0.0364	-0.0432	-0.0454	-0.0488	-0.0545	-0.0602	-0.0658	-0.0760	-0.0817	-0.0930
11.00	-0.0350	-0.0400	-0.0500	-0.0557	-0.0600	-0.0761	-0.0815	-0.0896	-0.1030	-0.1165	-0.1299	-0.1542	-0.1676	-0.1945
12.00	-0.0650	-0.0650	-0.0757	-0.0818	-0.0864	-0.0929	-0.0950	-0.1029	-0.1162	-0.1294	-0.1426	-0.1664	-0.1796	-0.2060
13.00	-0.0915	-0.0974	-0.1034	-0.1064	-0.1087	-0.1119	-0.1130	-0.1189	-0.1293	-0.1397	-0.1501	-0.2057	-0.2398	-0.3080
14.00	-0.1180	-0.1298	-0.1310	-0.1310	-0.1310	-0.1310	-0.1310	-0.1348	-0.1424	-0.1499	-0.1575	-0.2450	-0.3000	-0.4100
15.00	-0.1377	-0.1405	-0.1401	-0.1395	-0.1391	-0.1385	-0.1389	-0.1438	-0.1527	-0.1678	-0.1829	-0.2450	-0.3044	-0.4232
16.00	-0.1403	-0.1430	-0.1426	-0.1420	-0.1416	-0.1411	-0.1415	-0.1460	-0.1543	-0.1684	-0.1825	-0.2405	-0.2959	-0.4068
30.00	-0.1773	-0.1773	-0.1773	-0.1773	-0.1773	-0.1773	-0.1773	-0.1773	-0.1773	-0.1773	-0.1773	-0.1773	-0.1773	-0.1773
180.00	0.0144	0.0144	0.0144	0.0144	0.0144	0.0144	0.0144	0.0144	0.0144	0.0144	0.0144	0.0144	0.0144	0.0144

VR8 tab=0
for Boeing advanced tilt rotor blade, r = .84-.95
from M. Sheffler, Boeing Vertol, January 1983
also ATB at OARF, from Randy Smith, Boeing Vertol, March 1984

C81 table for the fourth blade segment (0.95–1.0 *R*):

```
 924 284 VR-8 0 TAB DCD=.0028 133420391437
        0.0000 0.3020 0.4010 0.5040 0.5600 0.5870 0.6170 0.6630 0.7130 0.7600 0.8200 0.9000 1.0000
-180.00 0.0053 0.0053 0.0053 0.0053 0.0053 0.0053 0.0053 0.0053 0.0053 0.0053 0.0053 0.0053 0.0053
 -30.00-1.0615-1.0615-1.0615-1.0615-1.0615-1.0615-1.0615-1.0615-1.0615-1.0615-1.0615-1.0615-1.0615
 -16.00-0.9868-0.9260-0.9352-0.9342-0.9360-0.9384-0.9302-0.9302-0.9648-0.9784-1.2975-1.6200-1.4800
 -14.00-0.9802-0.8890-0.9028-0.9014-0.9040-0.9076-0.8953-0.8953-0.9472-0.9676-1.1962-1.4300-1.2950
 -13.00-0.9769-0.8705-0.8866-0.8849-0.8880-0.8922-0.8779-0.8779-0.9384-0.9622-1.1456-1.3350-1.2025
 -12.00-0.9736-0.8520-0.8704-0.8685-0.8720-0.8768-0.8604-0.8604-0.9296-0.9568-1.0950-1.2400-1.1100
 -11.00-0.9703-0.8335-0.8542-0.8520-0.8560-0.8614-0.8430-0.8430-0.9208-0.9514-1.0444-1.1450-1.0175
 -10.00-0.9670-0.8150-0.8380-0.8356-0.8400-0.8460-0.8255-0.8255-0.9120-0.9460-0.9938-1.0500-0.9250
  -9.00-0.8609-0.7595-0.7840-0.7923-0.7867-0.7973-0.8062-0.8116-0.9071-0.9485-0.9431-0.9550-0.8325
  -8.00-0.7548-0.7040-0.7300-0.7490-0.7333-0.7487-0.7870-0.7978-0.9022-0.9510-0.8925-0.8600-0.7400
  -7.00-0.6487-0.6225-0.6460-0.6625-0.6800-0.7000-0.7018-0.7497-0.8501-0.8941-0.8419-0.7650-0.6475
  -6.00-0.5426-0.5410-0.5620-0.5760-0.5800-0.5963-0.6165-0.7016-0.7980-0.8373-0.7913-0.6700-0.5550
  -5.00-0.4365-0.4390-0.4615-0.4795-0.4800-0.4927-0.5183-0.5683-0.6432-0.6998-0.7406-0.5500-0.4625
  -4.00-0.3304-0.3370-0.3610-0.3830-0.3800-0.3890-0.4200-0.4350-0.4884-0.5623-0.6900-0.4300-0.3700
  -3.00-0.2243-0.2290-0.2464-0.2598-0.2575-0.2625-0.2848-0.2963-0.3338-0.3867-0.4812-0.3038-0.2775
  -2.00-0.1182-0.1210-0.1317-0.1365-0.1350-0.1360-0.1495-0.1575-0.1792-0.2112-0.2725-0.1775-0.1850
  -1.00-0.0121-0.0130-0.0171-0.0132-0.0125-0.0095-0.0143-0.0188-0.0246-0.0356-0.0038-0.0513-0.0925
   0.00 0.0940 0.0950 0.0975 0.1100 0.1100 0.1170 0.1210 0.1200 0.1300 0.1400 0.2650 0.0750-0.0000
   1.00 0.2004 0.2031 0.2100 0.2300 0.2357 0.2460 0.2544 0.2646 0.2871 0.3233 0.4700 0.2017 0.0925
   2.00 0.3067 0.3112 0.3225 0.3500 0.3614 0.3750 0.3879 0.4092 0.4442 0.5067 0.5700 0.3283 0.1850
   4.00 0.5195 0.5275 0.5475 0.5900 0.6129 0.6330 0.6547 0.6985 0.7585 0.7830 0.7167 0.6340 0.3700
   5.00 0.6258 0.6356 0.6600 0.7100 0.7386 0.7620 0.7881 0.8431 0.9031 0.8203 0.7900 0.8130 0.4625
   6.00 0.7322 0.7437 0.7725 0.8300 0.8643 0.8910 0.9216 0.9877 0.9525 0.8576 0.9007 0.9920 0.5550
   7.00 0.8385 0.8519 0.8850 0.9500 0.9900 1.0200 1.0550 1.0924 0.9961 0.8950 1.0113 1.1710 0.6475
   8.00 0.9449 0.9600 0.9590 1.0167 1.0900 1.1200 1.1620 1.1571 1.0830 0.9323 1.1220 1.3500 0.7400
   9.00 1.0300 1.0200 1.0100 1.0500 1.1500 1.1755 1.2400 1.2045 1.1700 1.0397 1.2327 1.4417 0.8325
  10.00 1.0300 1.0400 1.0225 1.0500 1.1000 1.1623 1.1467 1.1500 1.2233 1.1471 1.3433 1.5333 0.9250
  11.00 1.0300 1.0600 1.0350 1.0500 1.0840 1.1162 1.1300 1.1600 1.2480 1.2545 1.4540 1.6250 1.0175
  12.00 1.0300 1.0659 1.0475 1.0560 1.0680 1.0700 1.1133 1.1700 1.2440 1.3618 1.5647 1.7167 1.1100
  13.00 1.0300 1.0718 1.0612 1.0680 1.0643 1.0725 1.0967 1.1800 1.2400 1.4692 1.6753 1.8083 1.2025
  14.00 1.0300 1.0776 1.0750 1.0800 1.0729 1.0750 1.0800 1.1900 1.2867 1.5766 1.7860 1.9000 1.2950
  16.00 1.0300 1.0429 1.0333 1.0633 1.0900 1.0800 1.1067 1.2100 1.3800 1.8372 2.0073 2.0833 1.4800
  30.00 1.0615 1.0615 1.0615 1.0615 1.0615 1.0615 1.0615 1.0615 1.0615 1.0615 1.0615 1.0615 1.0615
 180.00 0.0053 0.0053 0.0053 0.0053 0.0053 0.0053 0.0053 0.0053 0.0053 0.0053 0.0053 0.0053 0.0053
```

	0.0000	0.2000	0.2500	0.3000	0.4000	0.5000	0.5580	0.5820	0.6000	0.6480
	0.6750	0.7100	0.7500	0.7750	0.8200	0.8400	0.8750	0.8900	0.9000	1.0000
-180.00	0.0262	0.0262	0.0262	0.0262	0.0262	0.0262	0.0262	0.0262	0.0262	0.0262
	0.0262	0.0262	0.0262	0.0262	0.0262	0.0262	0.0262	0.0262	0.0262	0.0262
-90.00	1.5602	1.5602	1.5602	1.5602	1.5602	1.5602	1.5602	1.5602	1.5602	1.5602
	1.5602	1.5602	1.5602	1.5602	1.5602	1.5602	1.5602	1.5602	1.5602	1.5602
-30.00	0.8224	0.8224	0.8224	0.8224	0.8224	0.8224	0.8224	0.8224	0.8224	0.8224
	0.8224	0.8224	0.8224	0.8224	0.8224	0.8224	0.8224	0.8224	0.8224	0.8224
-16.00	0.4747	0.4747	0.4747	0.4747	0.4747	0.4747	0.4747	0.4747	0.4747	0.4747
	0.4747	0.4747	0.4747	0.4747	0.4747	0.4747	0.4747	0.4747	0.4747	0.4747
-15.00	0.4422	0.4422	0.4422	0.4422	0.4422	0.4422	0.4422	0.4422	0.4422	0.4422
	0.4422	0.4422	0.4422	0.4422	0.4422	0.4422	0.4422	0.4422	0.4422	0.4422
-14.00	0.4084	0.4084	0.4084	0.4084	0.4084	0.4084	0.4084	0.4084	0.4084	0.4084
	0.4084	0.4084	0.4084	0.4084	0.4084	0.4084	0.4084	0.4084	0.4084	0.4084
-13.00	0.3732	0.3732	0.3732	0.3732	0.3732	0.3732	0.3732	0.3732	0.3732	0.3732
	0.3732	0.3732	0.3732	0.3732	0.3732	0.3732	0.3732	0.3732	0.3732	0.3732
-12.00	0.3365	0.3365	0.3365	0.3365	0.3365	0.3365	0.3365	0.3365	0.3365	0.3365
	0.3365	0.3365	0.3365	0.3365	0.3365	0.3365	0.3365	0.3365	0.3365	0.3365
-11.00	0.2983	0.2983	0.2983	0.2983	0.2983	0.2983	0.2983	0.2983	0.2983	0.2983
	0.2983	0.2983	0.2983	0.2983	0.2983	0.2983	0.2983	0.2983	0.2983	0.2983
-10.00	0.2449	0.2460	0.2463	0.2466	0.2472	0.2477	0.2490	0.2495	0.2493	0.2511
	0.2527	0.2547	0.2589	0.2621	0.2680	0.2706	0.2751	0.2771	0.2784	0.2914
-9.00	0.1916	0.1938	0.1943	0.1949	0.1960	0.1971	0.1996	0.2007	0.2004	0.2039
	0.2071	0.2111	0.2194	0.2259	0.2376	0.2429	0.2519	0.2559	0.2585	0.2845
-8.00	0.1382	0.1415	0.1424	0.1432	0.1449	0.1466	0.1503	0.1519	0.1514	0.1568
	0.1615	0.1676	0.1800	0.1897	0.2073	0.2151	0.2288	0.2346	0.2385	0.2776
-7.00	0.0849	0.0893	0.0904	0.0915	0.0937	0.0960	0.1009	0.1031	0.1025	0.1096
	0.1159	0.1240	0.1405	0.1535	0.1769	0.1874	0.2056	0.2134	0.2186	0.2707
-6.00	0.0315	0.0370	0.0384	0.0398	0.0426	0.0454	0.0516	0.0543	0.0535	0.0624
	0.0703	0.0804	0.1011	0.1173	0.1466	0.1597	0.1824	0.1922	0.1987	0.2638
-5.00	0.0221	0.0249	0.0256	0.0267	0.0290	0.0313	0.0349	0.0364	0.0362	0.0410
	0.0468	0.0559	0.0708	0.0845	0.1123	0.1226	0.1396	0.1469	0.1518	0.1843
-4.00	0.0128	0.0128	0.0128	0.0137	0.0154	0.0172	0.0182	0.0185	0.0188	0.0196
	0.0232	0.0313	0.0405	0.0516	0.0779	0.0856	0.0968	0.1016	0.1048	0.1048
-3.00	0.0116	0.0116	0.0116	0.0121	0.0130	0.0139	0.0143	0.0145	0.0147	0.0149
	0.0166	0.0207	0.0257	0.0314	0.0471	0.0542	0.0767	0.0864	0.0928	0.0928
-2.00	0.0105	0.0105	0.0105	0.0105	0.0105	0.0105	0.0105	0.0105	0.0105	0.0102
	0.0100	0.0101	0.0108	0.0113	0.0164	0.0228	0.0566	0.0711	0.0808	0.0808
-1.00	0.0106	0.0105	0.0104	0.0104	0.0103	0.0102	0.0102	0.0102	0.0102	0.0101
	0.0101	0.0101	0.0107	0.0110	0.0172	0.0331	0.0630	0.0758	0.0758	0.0758
0.00	0.0106	0.0103	0.0102	0.0101	0.0100	0.0098	0.0099	0.0100	0.0100	0.0102
	0.0102	0.0103	0.0115	0.0133	0.0270	0.0413	0.0663	0.0676	0.0684	0.0768

1.00	0.0098	0.0094	0.0094	0.0093	0.0091	0.0094	0.0096	0.0096	0.0097	0.0098
	0.0099	0.0100	0.0112	0.0183	0.0428	0.0525	0.0696	0.0769	0.0793	0.0793
2.00	0.0098	0.0096	0.0095	0.0094	0.0093	0.0095	0.0095	0.0095	0.0095	0.0097
	0.0099	0.0101	0.0139	0.0262	0.0563	0.0634	0.0758	0.0811	0.0847	0.0868
3.00	0.0103	0.0101	0.0101	0.0100	0.0099	0.0098	0.0098	0.0097	0.0097	0.0102
	0.0106	0.0120	0.0272	0.0429	0.0683	0.0752	0.0874	0.0926	0.0961	0.0978
4.00	0.0103	0.0101	0.0100	0.0099	0.0098	0.0100	0.0101	0.0102	0.0102	0.0103
	0.0124	0.0220	0.0526	0.0660	0.0829	0.0904	0.1035	0.1091	0.1128	0.1228
5.00	0.0105	0.0104	0.0104	0.0104	0.0103	0.0106	0.0108	0.0119	0.0126	0.0223
	0.0317	0.0474	0.0703	0.0817	0.0987	0.1062	0.1194	0.1251	0.1288	0.1528
6.00	0.0108	0.0108	0.0108	0.0108	0.0108	0.0112	0.0115	0.0136	0.0151	0.0342
	0.0510	0.0728	0.0880	0.0975	0.1145	0.1221	0.1354	0.1411	0.1449	0.1828
7.00	0.0143	0.0128	0.0137	0.0147	0.0166	0.0175	0.0222	0.0264	0.0296	0.0525
	0.0694	0.0913	0.1115	0.1242	0.1469	0.1570	0.1747	0.1822	0.1873	0.2378
8.00	0.0178	0.0148	0.0167	0.0186	0.0224	0.0237	0.0329	0.0393	0.0441	0.0708
	0.0878	0.1099	0.1351	0.1509	0.1793	0.1919	0.2140	0.2234	0.2297	0.2928
9.00	0.0316	0.0376	0.0405	0.0433	0.0490	0.0534	0.0720	0.0810	0.0878	0.1086
	0.1244	0.1485	0.1678	0.1824	0.2105	0.2230	0.2448	0.2542	0.2604	0.3228
10.00	0.0453	0.0605	0.0642	0.0680	0.0756	0.0832	0.1112	0.1227	0.1314	0.1464
	0.1610	0.1871	0.2005	0.2139	0.2417	0.2540	0.2756	0.2849	0.2911	0.3528
11.00	0.0715	0.0971	0.1035	0.1099	0.1227	0.1340	0.1523	0.1599	0.1656	0.1822
	0.1946	0.2168	0.2411	0.2566	0.2848	0.2974	0.3194	0.3288	0.3350	0.3978
12.00	0.0978	0.1338	0.1428	0.1518	0.1698	0.1848	0.1935	0.1971	0.1998	0.2180
	0.2283	0.2466	0.2817	0.2993	0.3280	0.3407	0.3631	0.3726	0.3790	0.4428
13.00	0.1311	0.1711	0.1811	0.1911	0.2058	0.2178	0.2248	0.2276	0.2298	0.2592
	0.2757	0.3005	0.3382	0.3518	0.3709	0.3794	0.3943	0.4007	0.4049	0.4475
14.00	0.1645	0.2085	0.2195	0.2305	0.2418	0.2508	0.2560	0.2582	0.2598	0.3004
	0.3232	0.3544	0.3948	0.4043	0.4139	0.4181	0.4256	0.4287	0.4309	0.4521
15.00	0.1978	0.2458	0.2578	0.2698	0.2778	0.2838	0.2873	0.2887	0.2898	0.3415
	0.3706	0.4083	0.4514	0.4568	0.4568	0.4568	0.4568	0.4568	0.4568	0.4568
16.00	0.2289	0.2737	0.2849	0.2961	0.3036	0.3092	0.3125	0.3138	0.3148	0.3631
	0.3902	0.4254	0.4656	0.4707	0.4707	0.4707	0.4707	0.4707	0.4707	0.4707
30.00	0.6650	0.6650	0.6650	0.6650	0.6650	0.6650	0.6650	0.6650	0.6650	0.6650
	0.6650	0.6650	0.6650	0.6650	0.6650	0.6650	0.6650	0.6650	0.6650	0.6650
90.00	1.5602	1.5602	1.5602	1.5602	1.5602	1.5602	1.5602	1.5602	1.5602	1.5602
	1.5602	1.5602	1.5602	1.5602	1.5602	1.5602	1.5602	1.5602	1.5602	1.5602
180.00	0.0262	0.0262	0.0262	0.0262	0.0262	0.0262	0.0262	0.0262	0.0262	0.0262
	0.0262	0.0262	0.0262	0.0262	0.0262	0.0262	0.0262	0.0262	0.0262	0.0262

	0.0000	0.3000	0.4000	0.4570	0.5000	0.5600	0.5800	0.6100	0.6600	0.7100	0.7600	0.8500	0.9000	1.0000
-180.00	0.0144	0.0144	0.0144	0.0144	0.0144	0.0144	0.0144	0.0144	0.0144	0.0144	0.0144	0.0144	0.0144	0.0144
-30.00	0.1800	0.1800	0.1800	0.1800	0.1800	0.1800	0.1800	0.1800	0.1800	0.1800	0.1800	0.1800	0.1800	0.1800
-16.00	0.0946	0.0946	0.0946	0.0987	0.1018	0.1061	0.1076	0.1097	0.1133	0.1169	0.1205	0.1743	0.2042	0.2640
-15.00	0.0885	0.0885	0.0885	0.0929	0.0962	0.1008	0.1024	0.1047	0.1085	0.1124	0.1163	0.1739	0.2060	0.2700
-14.00	0.0824	0.0824	0.0824	0.0871	0.0906	0.0955	0.0972	0.0997	0.1038	0.1079	0.1120	0.1735	0.2077	0.2760
-13.00	0.0763	0.0763	0.0763	0.0813	0.0851	0.0902	0.0920	0.0947	0.0990	0.1034	0.1078	0.1731	0.2094	0.2820
-12.00	0.0702	0.0702	0.0702	0.0755	0.0795	0.0850	0.0869	0.0896	0.0942	0.0989	0.1035	0.1727	0.2111	0.2880
-11.00	0.0641	0.0641	0.0641	0.0697	0.0739	0.0797	0.0817	0.0846	0.0895	0.0944	0.0993	0.1723	0.2129	0.2940
-10.00	0.0580	0.0580	0.0580	0.0639	0.0683	0.0744	0.0765	0.0796	0.0847	0.0899	0.0950	0.1719	0.2146	0.3000
-9.00	0.0290	0.0320	0.0329	0.0364	0.0423	0.0505	0.0532	0.0573	0.0641	0.0709	0.0923	0.1646	0.2047	0.2850
-8.00	-0.0000	0.0059	0.0079	0.0090	0.0163	0.0265	0.0299	0.0350	0.0435	0.0520	0.0896	0.1572	0.1948	0.2700
-7.00	-0.0050	-0.0020	-0.0011	-0.0005	0.0032	0.0083	0.0100	0.0125	0.0126	0.0201	0.0592	0.1296	0.1774	0.1850
-6.00	-0.0100	-0.0100	-0.0100	-0.0100	-0.0100	-0.0100	-0.0100	-0.0100	-0.0182	-0.0118	0.0288	0.1019	0.1600	0.1000
-5.00	-0.0100	-0.0100	-0.0100	-0.0100	-0.0100	-0.0103	-0.0110	-0.0119	-0.0176	-0.0145	0.0057	0.0422	0.0711	0.0410
-4.00	-0.0100	-0.0100	-0.0100	-0.0100	-0.0100	-0.0106	-0.0119	-0.0138	-0.0170	-0.0171	-0.0173	-0.0176	-0.0177	-0.0180
-3.00	-0.0137	-0.0113	-0.0105	-0.0105	-0.0105	-0.0108	-0.0115	-0.0124	-0.0141	-0.0142	-0.0143	-0.0146	-0.0147	-0.0150
-2.00	-0.0174	-0.0126	-0.0110	-0.0110	-0.0110	-0.0110	-0.0110	-0.0110	-0.0111	-0.0113	-0.0114	-0.0116	-0.0117	-0.0120
-1.00	-0.0155	-0.0134	-0.0127	-0.0127	-0.0128	-0.0128	-0.0129	-0.0129	-0.0130	-0.0131	-0.0132	-0.0133	-0.0134	-0.0135
0.00	-0.0135	-0.0141	-0.0143	-0.0145	-0.0146	-0.0147	-0.0147	-0.0148	-0.0149	-0.0150	-0.0151	-0.0153	-0.0154	-0.0156
1.00	-0.0151	-0.0158	-0.0160	-0.0162	-0.0163	-0.0164	-0.0165	-0.0165	-0.0166	-0.0167	-0.0169	-0.0171	-0.0172	-0.0174
2.00	-0.0168	-0.0175	-0.0178	-0.0179	-0.0180	-0.0181	-0.0182	-0.0183	-0.0184	-0.0185	-0.0186	-0.0188	-0.0190	-0.0192
3.00	-0.0179	-0.0185	-0.0187	-0.0188	-0.0189	-0.0190	-0.0191	-0.0191	-0.0192	-0.0193	-0.0194	-0.0196	-0.0197	-0.0199
4.00	-0.0190	-0.0195	-0.0196	-0.0197	-0.0198	-0.0199	-0.0199	-0.0200	-0.0201	-0.0201	-0.0202	-0.0204	-0.0204	-0.0206
5.00	-0.0210	-0.0203	-0.0201	-0.0199	-0.0198	-0.0197	-0.0197	-0.0197	-0.0198	-0.0198	-0.0199	-0.0199	-0.0200	-0.0200
6.00	-0.0230	-0.0211	-0.0205	-0.0201	-0.0199	-0.0195	-0.0195	-0.0195	-0.0195	-0.0195	-0.0195	-0.0195	-0.0195	-0.0195
7.00	-0.0262	-0.0214	-0.0198	-0.0189	-0.0185	-0.0185	-0.0185	-0.0186	-0.0188	-0.0189	-0.0191	-0.0193	-0.0195	-0.0197
8.00	-0.0295	-0.0218	-0.0192	-0.0177	-0.0171	-0.0174	-0.0176	-0.0177	-0.0180	-0.0183	-0.0186	-0.0191	-0.0194	-0.0200
9.00	-0.0295	-0.0229	-0.0222	-0.0246	-0.0267	-0.0303	-0.0315	-0.0333	-0.0363	-0.0392	-0.0422	-0.0476	-0.0505	-0.0565
10.00	-0.0295	-0.0240	-0.0251	-0.0316	-0.0364	-0.0432	-0.0454	-0.0488	-0.0545	-0.0602	-0.0658	-0.0760	-0.0817	-0.0930
11.00	-0.0350	-0.0400	-0.0500	-0.0557	-0.0600	-0.0761	-0.0815	-0.0896	-0.1030	-0.1165	-0.1299	-0.1542	-0.1676	-0.1945
12.00	-0.0650	-0.0650	-0.0757	-0.0818	-0.0864	-0.0929	-0.0950	-0.1029	-0.1162	-0.1294	-0.1426	-0.1664	-0.1796	-0.2060
13.00	-0.0915	-0.0974	-0.1034	-0.1064	-0.1087	-0.1119	-0.1130	-0.1189	-0.1293	-0.1397	-0.1501	-0.2057	-0.2398	-0.3080
14.00	-0.1180	-0.1298	-0.1310	-0.1310	-0.1310	-0.1310	-0.1310	-0.1348	-0.1424	-0.1499	-0.1575	-0.2450	-0.3000	-0.4100
15.00	-0.1377	-0.1405	-0.1401	-0.1395	-0.1391	-0.1385	-0.1389	-0.1438	-0.1527	-0.1678	-0.1829	-0.2450	-0.3044	-0.4232
16.00	-0.1403	-0.1430	-0.1426	-0.1420	-0.1416	-0.1411	-0.1415	-0.1460	-0.1543	-0.1684	-0.1825	-0.2405	-0.2959	-0.4068
30.00	-0.1773	-0.1773	-0.1773	-0.1773	-0.1773	-0.1773	-0.1773	-0.1773	-0.1773	-0.1773	-0.1773	-0.1773	-0.1773	-0.1773
180.00	0.0144	0.0144	0.0144	0.0144	0.0144	0.0144	0.0144	0.0144	0.0144	0.0144	0.0144	0.0144	0.0144	0.0144

VR8, tab=0
for Boeing advanced tilt rotor blade, r = .95-1.0
from M. Sheffler, Boeing Vertol, January 1983
also ATB at OARF, from Randy Smith, Boeing Vertol, March 1984

APPENDIX B: XV-15 CONTROL-SYSTEM STIFFNESS MATRICES

In the C97 model of the ATBs, as in nearly all models of the XV-15 with steel blades, the control-system stiffness was set to a uniform value, independent of control position. This was input as CAMRAD variables KT0 = KTC = KTR = 13,900 ft·lb/rad. For the ATB analysis, CAMRAD was extended to include a full 3 × 3 cross-coupling matrix, input as KPITCH. KT0, KTC, and KTR were set equal to KPITCH(1,1), varying with collective angle.

Complete Matrices (No Shims)

From reference 6, the full stiffness matrix may be given as

$$\begin{bmatrix} \theta_0 \\ \theta_{1C} \\ \theta_{1S} \end{bmatrix} = \begin{bmatrix} 6.5890 & -1.0937 & -1.0937 \\ -1.9627 & 6.8167 - \dfrac{\theta_{75}}{0.349} & 0 \\ -1.9627 & 0 & 7.0518 - \dfrac{\theta_{75}}{0.349} \end{bmatrix} \times \begin{bmatrix} M_0 \\ M_{1C} \\ M_{1S} \end{bmatrix} \div \left[1.11 \times 10^5 \cos^2(\theta_{75} - 0.342)\right]$$

where

θ_0 = collective pitch measured at the blade root, rad

θ_{1C} = lateral cyclic pitch, rad

θ_{1S} = longitudinal cyclic pitch, rad

θ_{75} = collective pitch measured at 75% R, rad

M_0 = collective pitch moment, ft·lb

M_{1C} = lateral cyclic moment, ft·lb

M_{1S} = longitudinal cyclic moment, ft·lb

For the analyses reported herein, the matrix was evaluated at 5° increments. The range of collective trim values was typically about 35° to 50°, measured at 75% R.

CAMRAD actually requires the inverse of this matrix as input data, that is, the elements of K in

$$\begin{bmatrix} M_0 \\ M_{1C} \\ M_{1S} \end{bmatrix} = [K] \times \begin{bmatrix} \theta_0 \\ \theta_{1C} \\ \theta_{1S} \end{bmatrix}$$

Matrices for Shims

The stiffness matrix for the shimmed control system is

$$\begin{bmatrix} \theta_0 \\ \theta_{1C} \\ \theta_{1S} \end{bmatrix} = \begin{bmatrix} 4.47 & -0.113 & -0.113 \\ 0 & 5.72 - \dfrac{\theta_{75}}{0.349} & 0 \\ 0 & 0 & 5.96 - \dfrac{\theta_{75}}{0.349} \end{bmatrix} \times \begin{bmatrix} M_0 \\ M_{1C} \\ M_{1S} \end{bmatrix} \div \left[1.11 \times 10^5 \cos^2(\theta_{75} - 0.342)\right]$$

The small, off-diagonal elements should ideally be zero; in the matrices actually used, they were so set on the assumption that non-zero values represent errors in the stiffness measurements. This was felt to be justified because the magnitude of the off-diagonal elements is less than what would result from known errors in the measurements. Trimmed collective values ranged from 35° to 50°, the same as for the full stiffness matrices.

REFERENCES

1. Alexander, H. R.; Maisel, M. D.; and Giulianetti, D. J.: The Development of Advanced Technology Blades for Tiltrotor Aircraft. Paper No. 39, 11th European Rotorcraft Forum, London, England, Sept. 1985.

2. Smith, K. W.; Alexander, H. R.; and Maisel, M. D.: Design Aspects of the XV-15 Advanced Technology Blade Program. Presented at the 41st Annual National Forum of the American Helicopter Society, Ft. Worth, Tex., 1985.

3. McVeigh, M. A.; Rosenstein, H. J.; and McHugh, F. J.: Aerodynamic Design of the XV-15 Advanced Composite Tilt Rotor Blade. Presented at the 39th Annual National Forum of the American Helicopter Society, St. Louis, Mo., May 1983.

4. Felker, F. F.; Young, L. A.; and Signor, D. B.: Performance and Loads Data from a Hover Test of a Full-Scale Advanced Technology XV-15 Rotor. NASA TM-86854, 1986.

5. Johnson, W.: CAMRAD/JA. A Comprehensive Analytical Model of Rotorcraft Aerodynamics and Dynamics. Vols. I and II. Johnson Aeronautics, Palo Alto, Calif., 1988.

6. Totah, J. J.; and Madden, J. F.: Rotor and Control System Loads Analysis of the XV-15 with the Advanced Technology Blades. Presented at the AHS National Technical Specialists' Meeting on Innovations in Rotorcraft Test Technologies for the 90's, Scottsdale, Ariz., Oct. 1990.

7. Johnson, W.: An Assessment of the Capability to Calculate Tilting Prop-Rotor Aircraft Performance, Loads, and Stability. NASA TP-2291, 1984.

8. Maisel, M. D., ed.: Tilt Rotor Research Aircraft Familiarization Document. NASA TM X-62, 407, 1975.

9. Arrington, W. L.; Kumpel, M.; Marr, R. L.; and McEntire, K. G.: XV-15 Tilt Rotor Research Aircraft Flight Test Data Report. Vol. II. Performance and Handling Qualities. NASA CR-177406, 1985. Also USAAVSCOM TR-86-A-1, June 1985.

10. XV-15 Flight Manual. Bell Helicopter Textron Report TP-78-XV-15-1, Aug. 1980.

11. Ferguson, S. W.: A Mathematical Model for Real-Time Flight Simulation of a Generic Tilt-Rotor Aircraft. NASA CR-166536, 1988.

Table 1. ATB configurations flown through March 1991

	Original control system	Shimmed control system
Twisted tips	1° Sweep	1° Sweep
Zero-twist tips	(No flights)	1° Sweep and 0° sweep

Table 2. Stability boundaries for ATB configurations analyzed at 80% rotor speed (481 rpm)

Configuration	Boundary for critical mode,[a] KTAS			
	Original XA[b]		Zero XA	
	Symmetric	Antisymmetric	Symmetric	Antisymmetric
1° Sweep, no shims, twisted tips	>350	309	>350	308
1° Sweep, shims, twisted tips	281	>350	312	>350
1° Sweep, shims, zero-twist tips	282	>350	302	>350
0° Sweep, shims, zero-twist tips	274	>350	293	>350

[a]The unstable mode was always a coupled collective-torsion/drive-train mode; values are interpolated between points calculated at 25-knot increments. Extrapolation above 350 KTAS is not considered reliable.
[b]Aerodynamic-center offset, steady and unsteady.

Table 3. Calculated blade frequencies[a] for 1° sweep and twisted tips, at 80% rotor speed (481 rpm) and 200 KTAS

Blade mode	Control stiffness matrix		
	No matrix[b]	Full matrix	Shim matrix
β_0 (lag)	1.280	1.282	1.285
β_2 (flap)	1.987	1.986	1.984
β_3 (flap/lag)	4.434	4.434	4.436
β_4 (flap)	8.293	8.293	8.293
θ_0	3.421	3.876	4.399
θ_2	10.515	10.515	10.515

[a]Nondimensional frequency, per rev.
[b]KT0 = KTC = KTR = 13,900 ft·lb/rad.

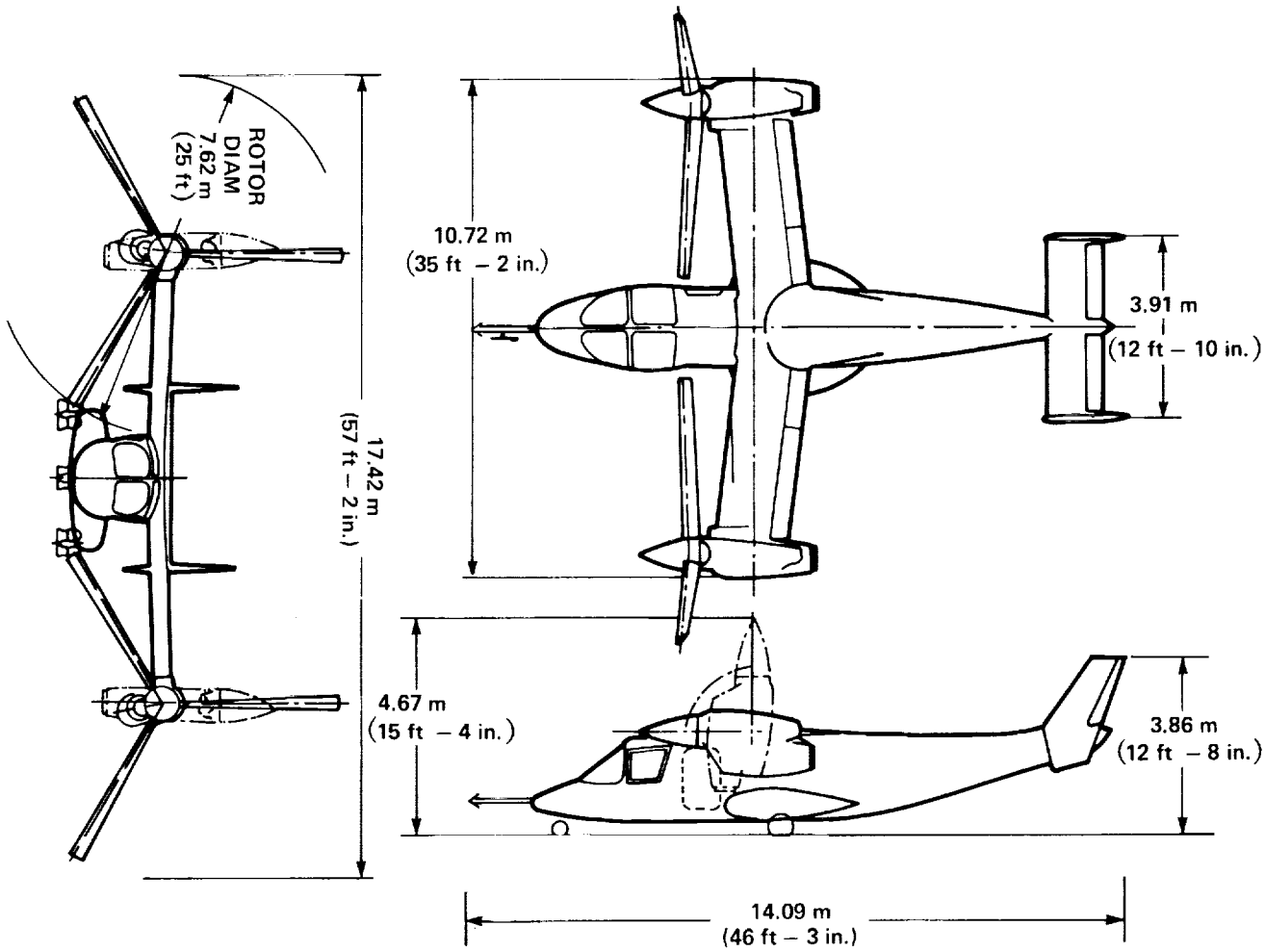

Figure 1. Three-view of the XV-15 Tiltrotor Research Aircraft.

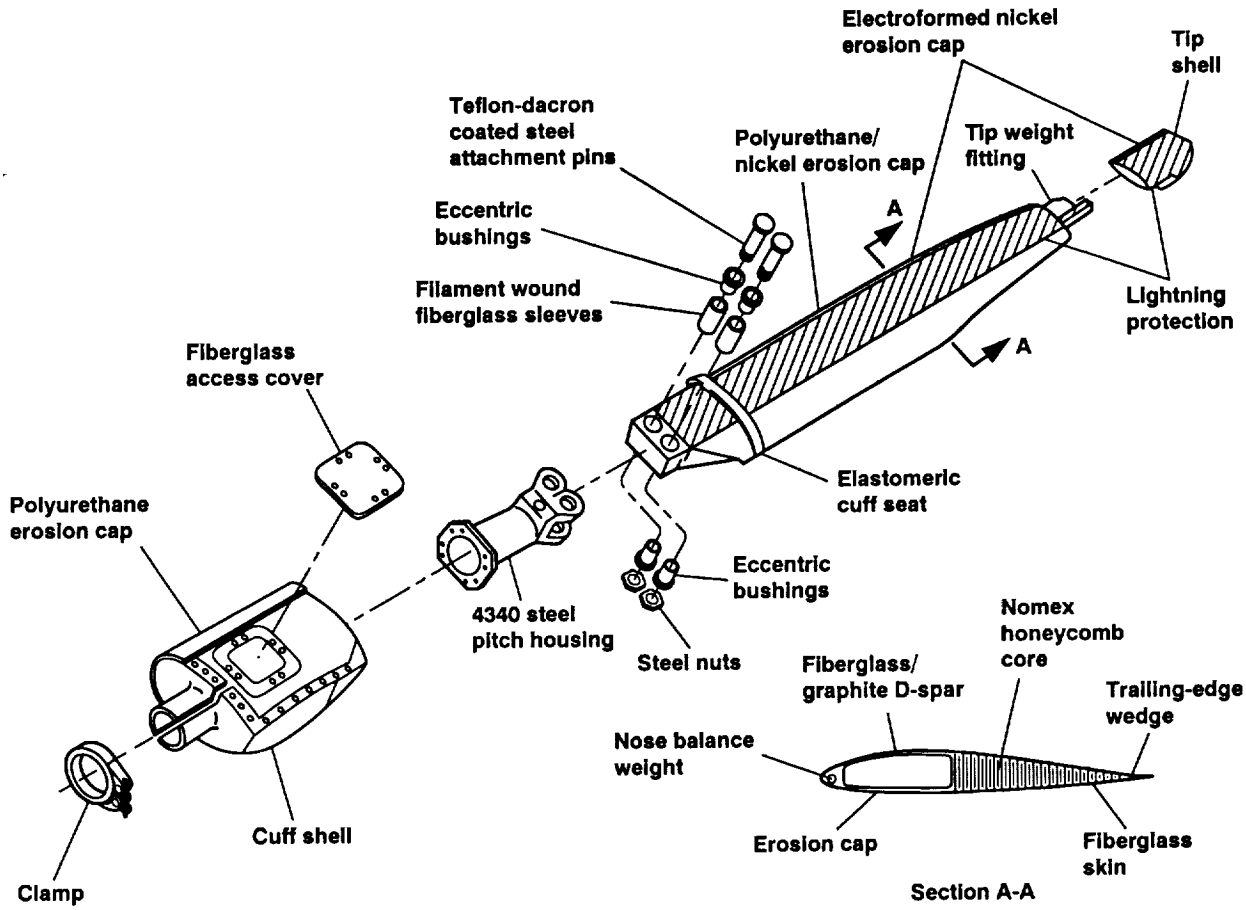

Figure 2. Structural assembly of the XV-15 Advanced Technology Blade.

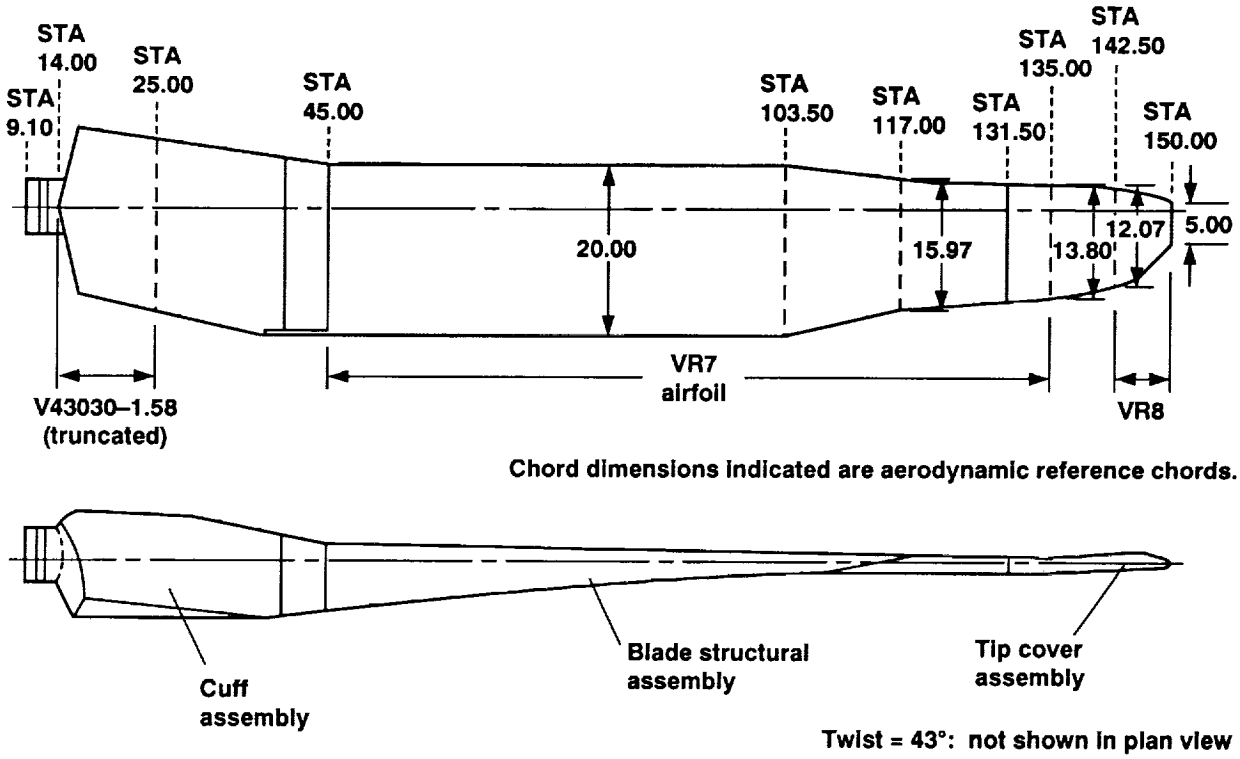

Figure 3. Planform and airfoil locations of the Advanced Technology Blade.

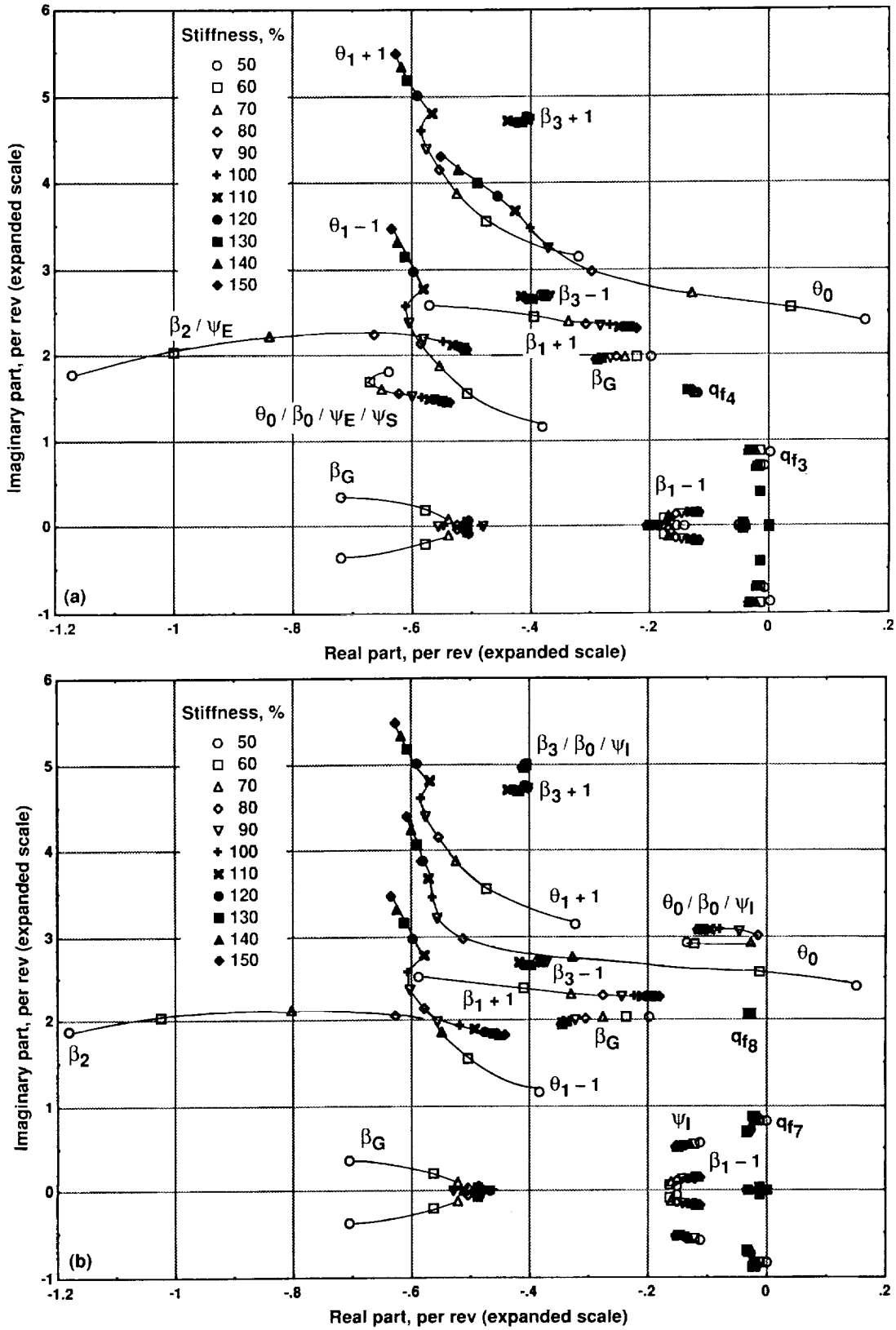

Figure 4. Eigenvalues for control-system stiffness variations (50-150% of 13,900 ft·lb/rad). C97 model with additional flutter-solution degrees of freedom; 86% rotor speed at 250 KTAS. (a) Symmetric modes. (b) Antisymmetric modes.

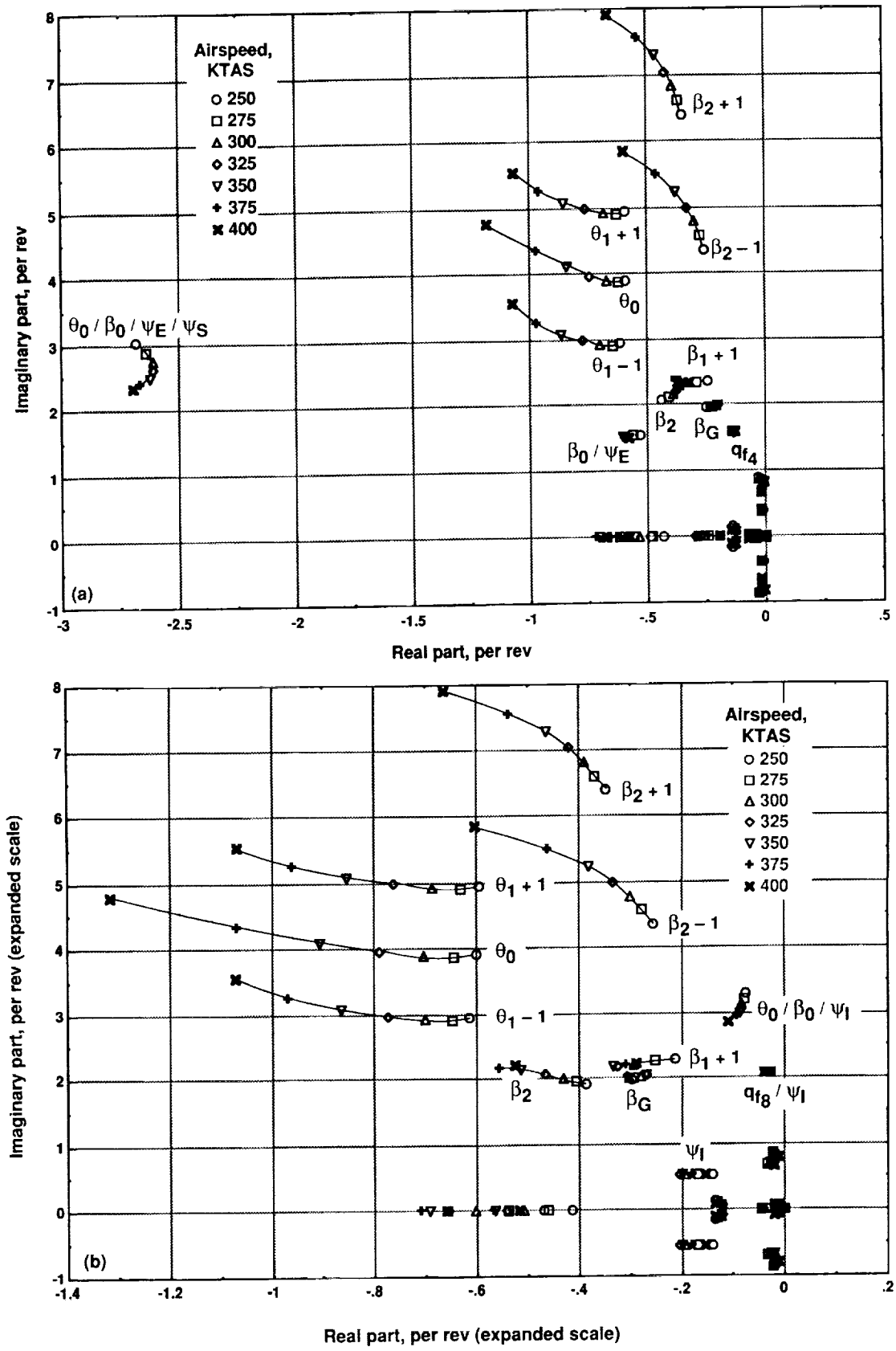

Figure 5. Eigenvalues for original C97 model; 250-400 KTAS speed variation at 86% rotor speed. (a) Symmetric modes. (b) Antisymmetric modes.

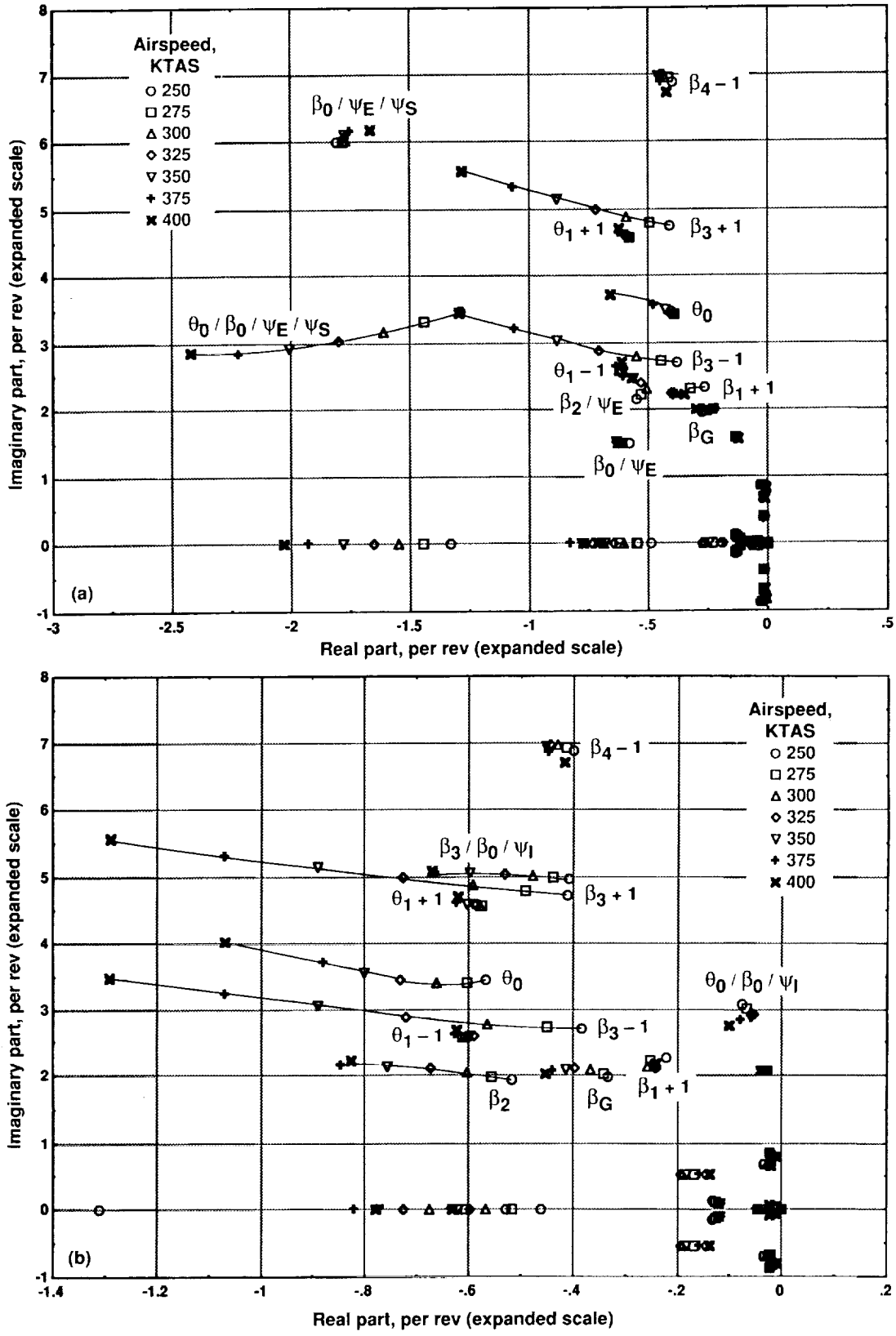

Figure 6. Eigenvalues for C97 model with additional flutter-solution degrees of freedom; 250-400 KTAS speed variation at 86% rotor speed. (a) Symmetric modes. (b) Antisymmetric modes.

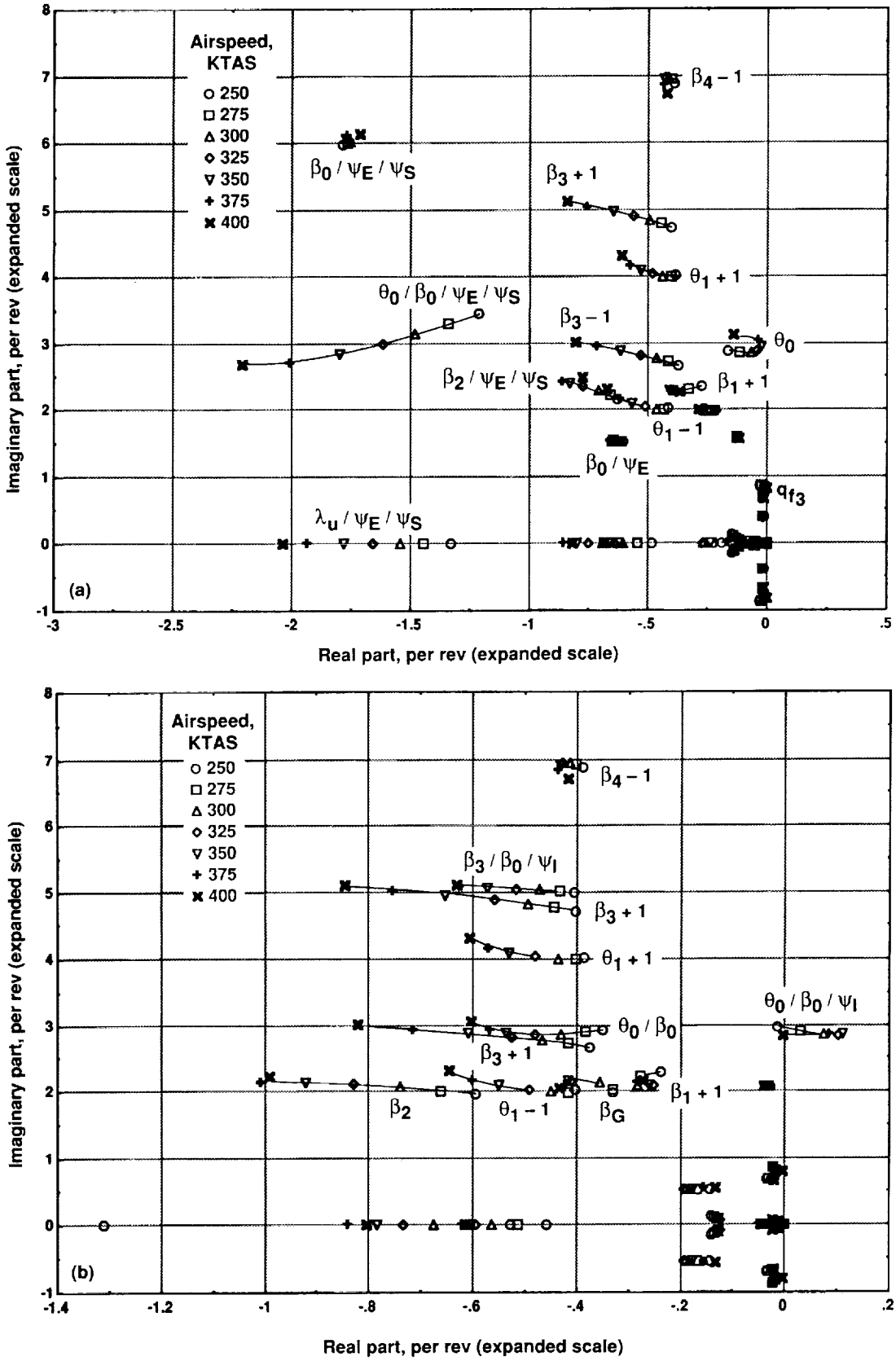

Figure 7. Eigenvalues for C97 model with increased cuff inertia and additional flutter-solution degrees of freedom; 250-400 KTAS speed variation at 86% rotor speed. (a) Symmetric modes. (b) Antisymmetric modes.

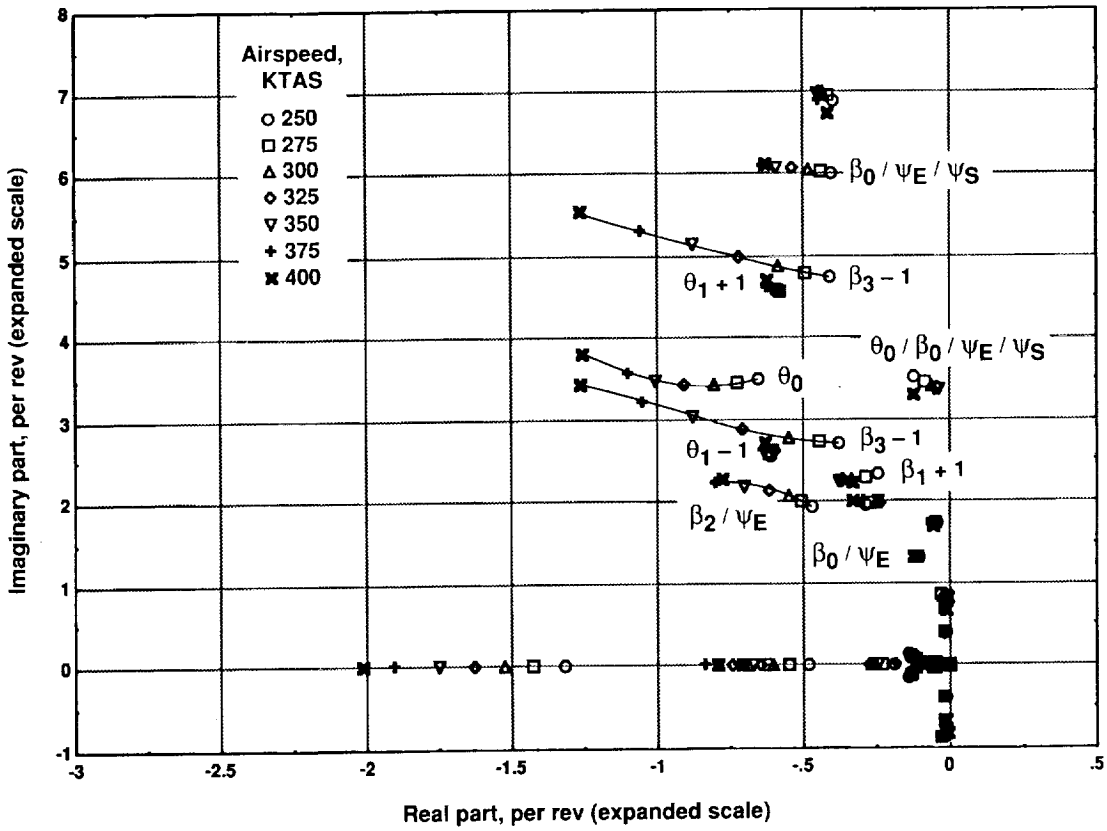

Figure 8. Eigenvalues for C97 model with corrected engine-shaft damping and additional flutter-solution degrees of freedom; 250-400 KTAS speed variation at 86% rotor speed (symmetric modes only).

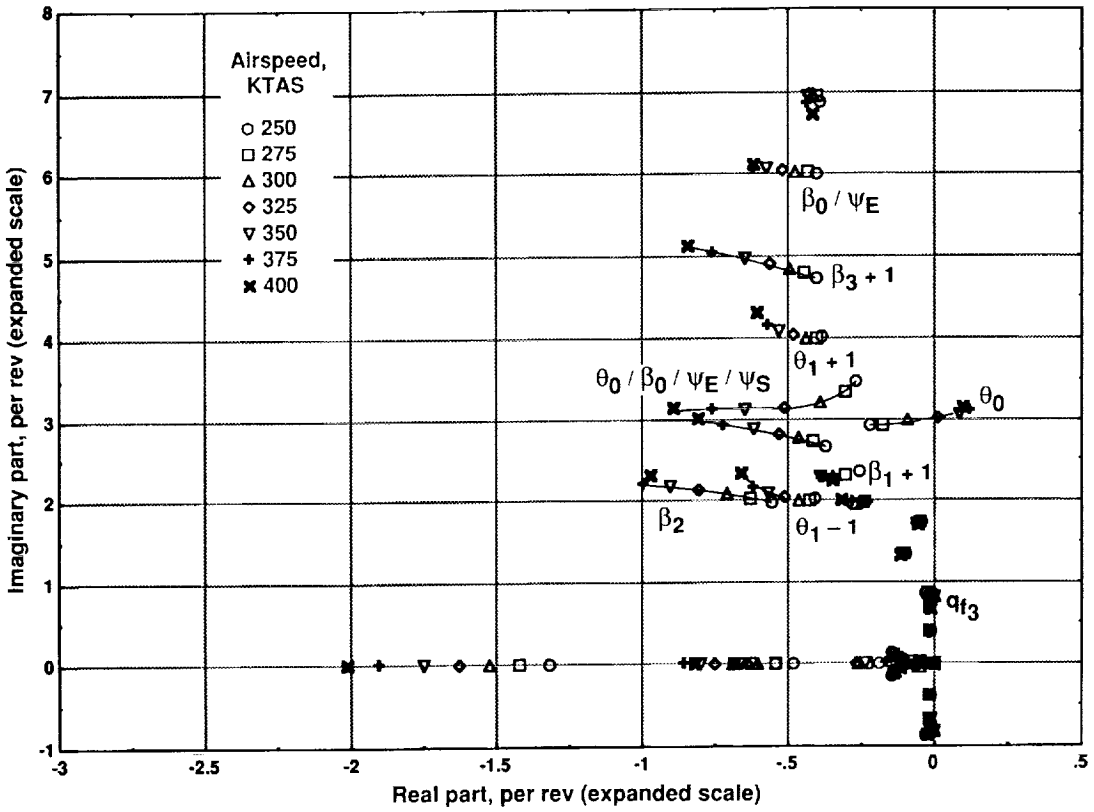

Figure 9. Eigenvalues for C97 model with increased cuff inertia, corrected engine-shaft damping, and additional flutter-solution degrees of freedom; 250-400 KTAS speed variation at 86% rotor speed (symmetric modes only).

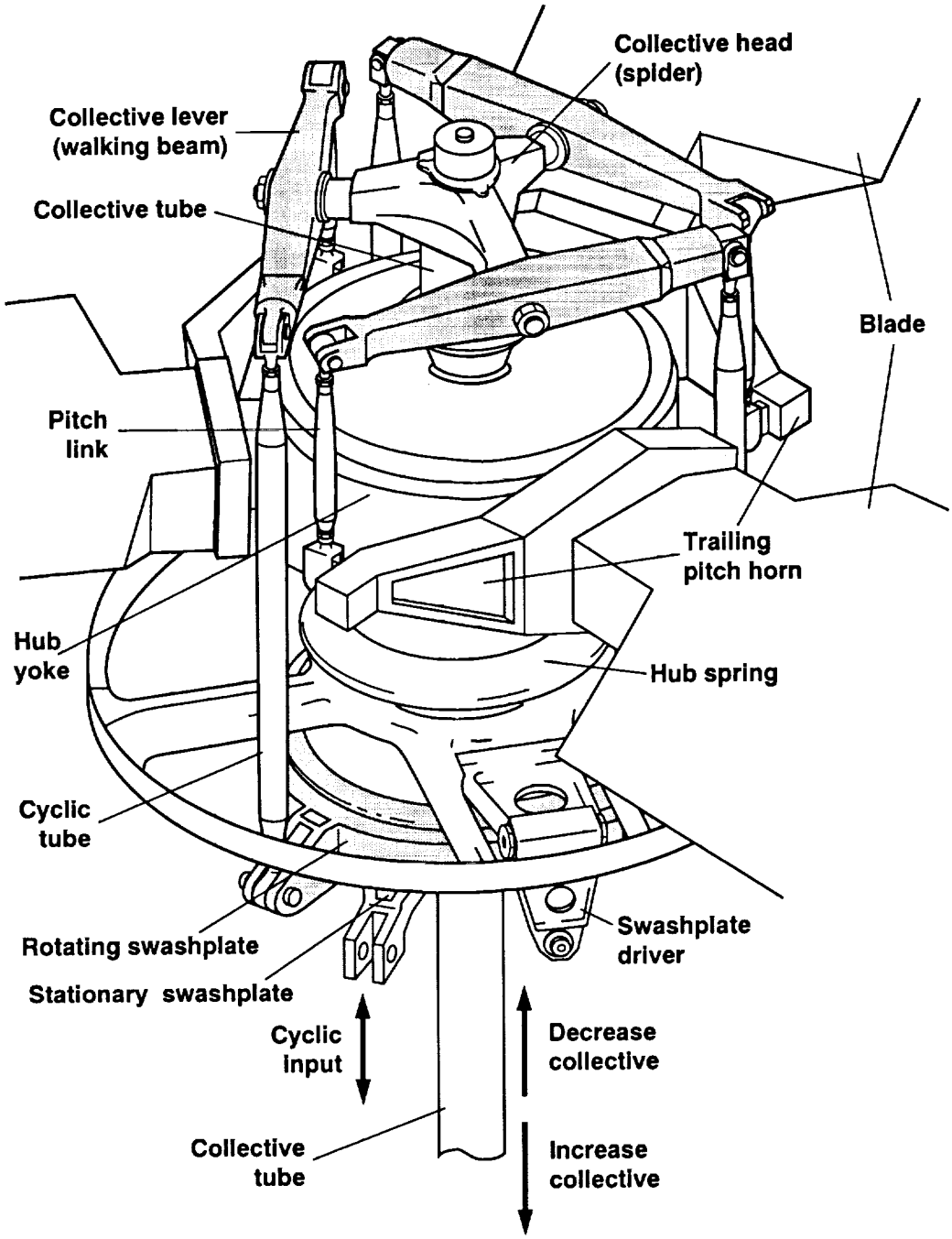

Figure 10. Simplified arrangement of the XV-15 rotor control system (a complete set of control tubes is shown for only one blade).

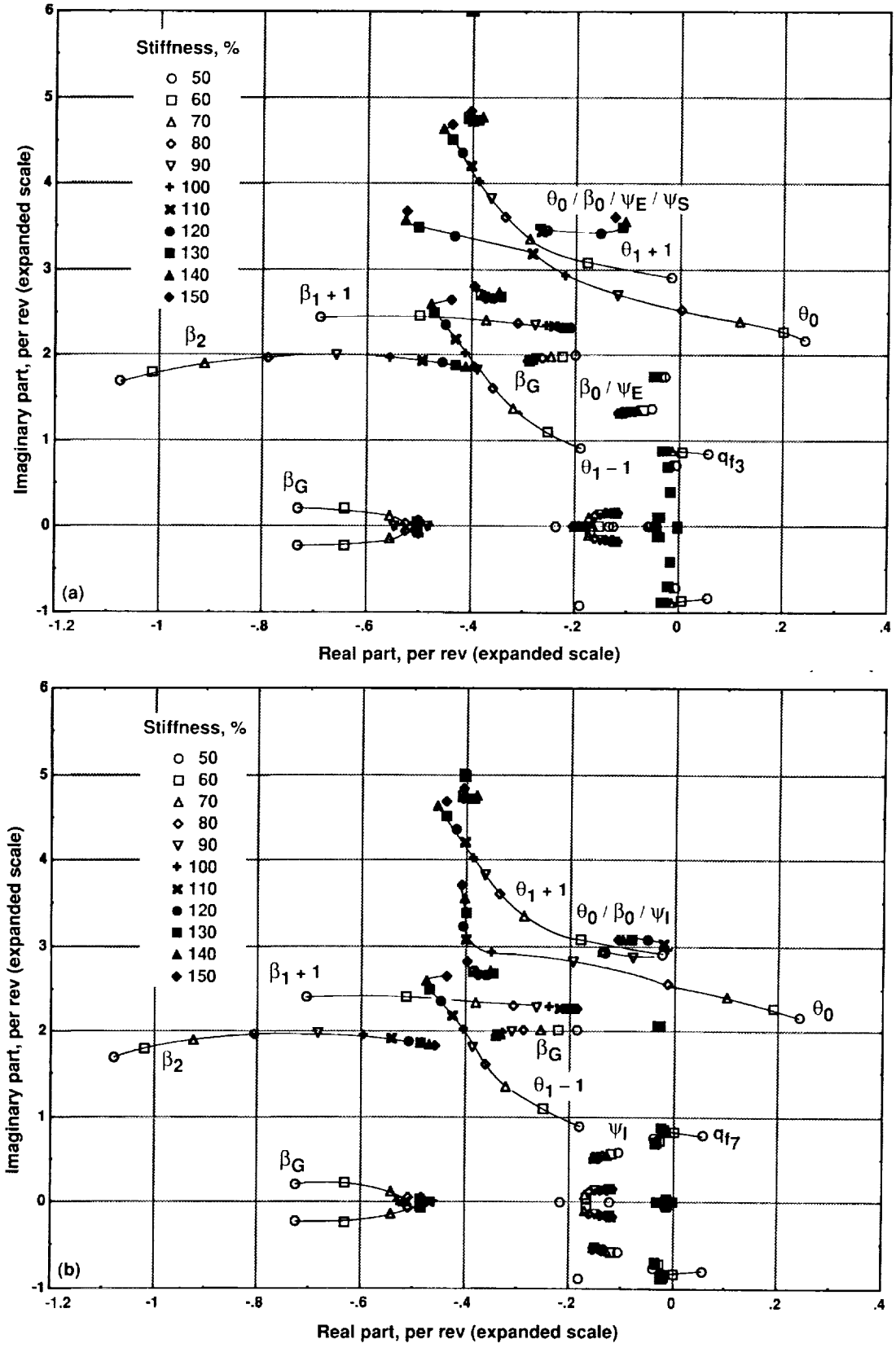

Figure 11. Eigenvalues for control-system stiffness variations (50-150% of 13,900 ft·lb/rad). C97 model with increased cuff inertia, corrected engine-shaft damping, and additional flutter-solution degrees of freedom; 86% rotor speed at 250 KTAS. (a) Symmetric modes. (b) Antisymmetric modes.

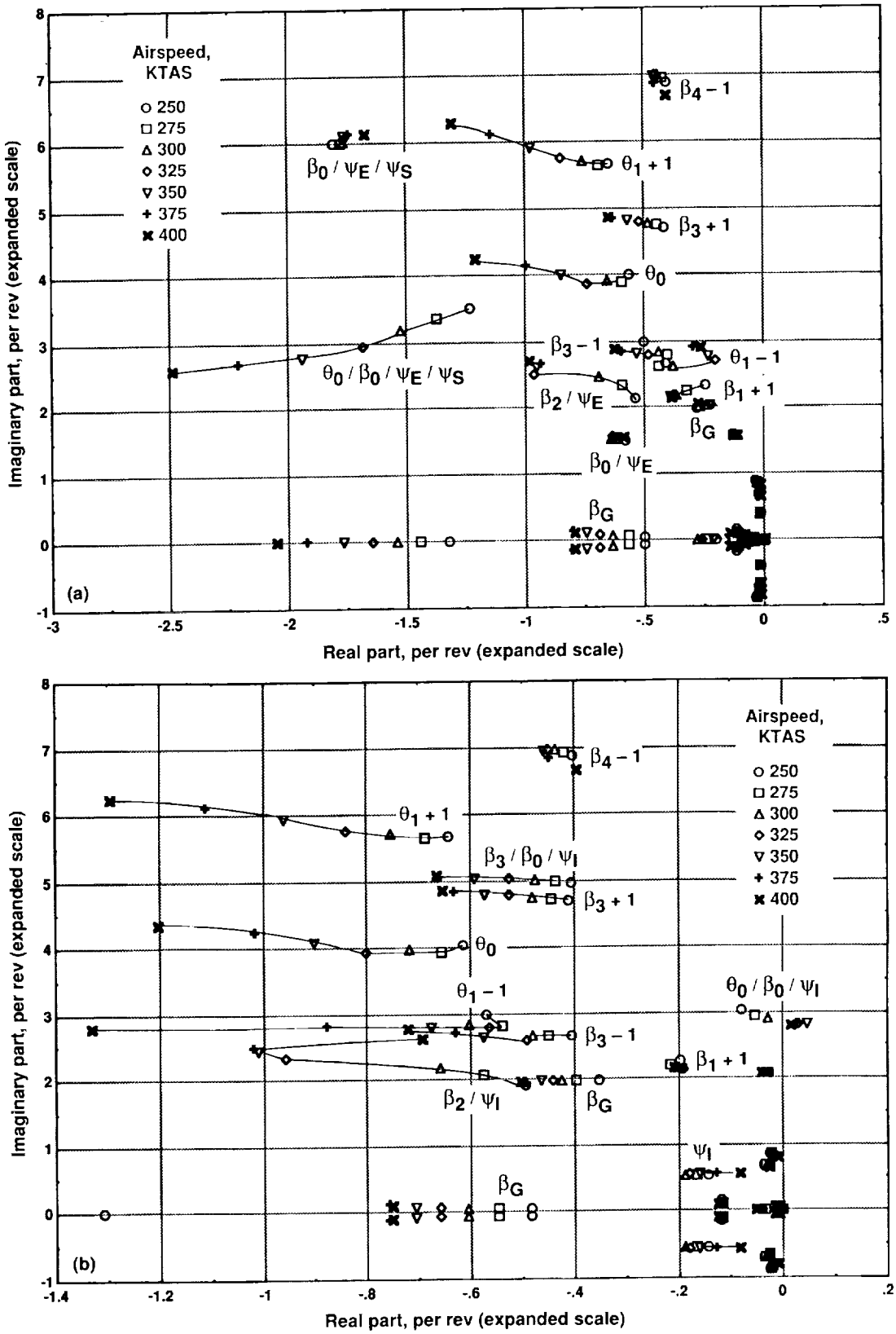

Figure 12. Eigenvalues for C97 model with full control-system stiffness matrices and additional flutter-solution degrees of freedom; 250-400 KTAS speed variation at 86% rotor speed. (a) Symmetric modes. (b) Antisymmetric modes.

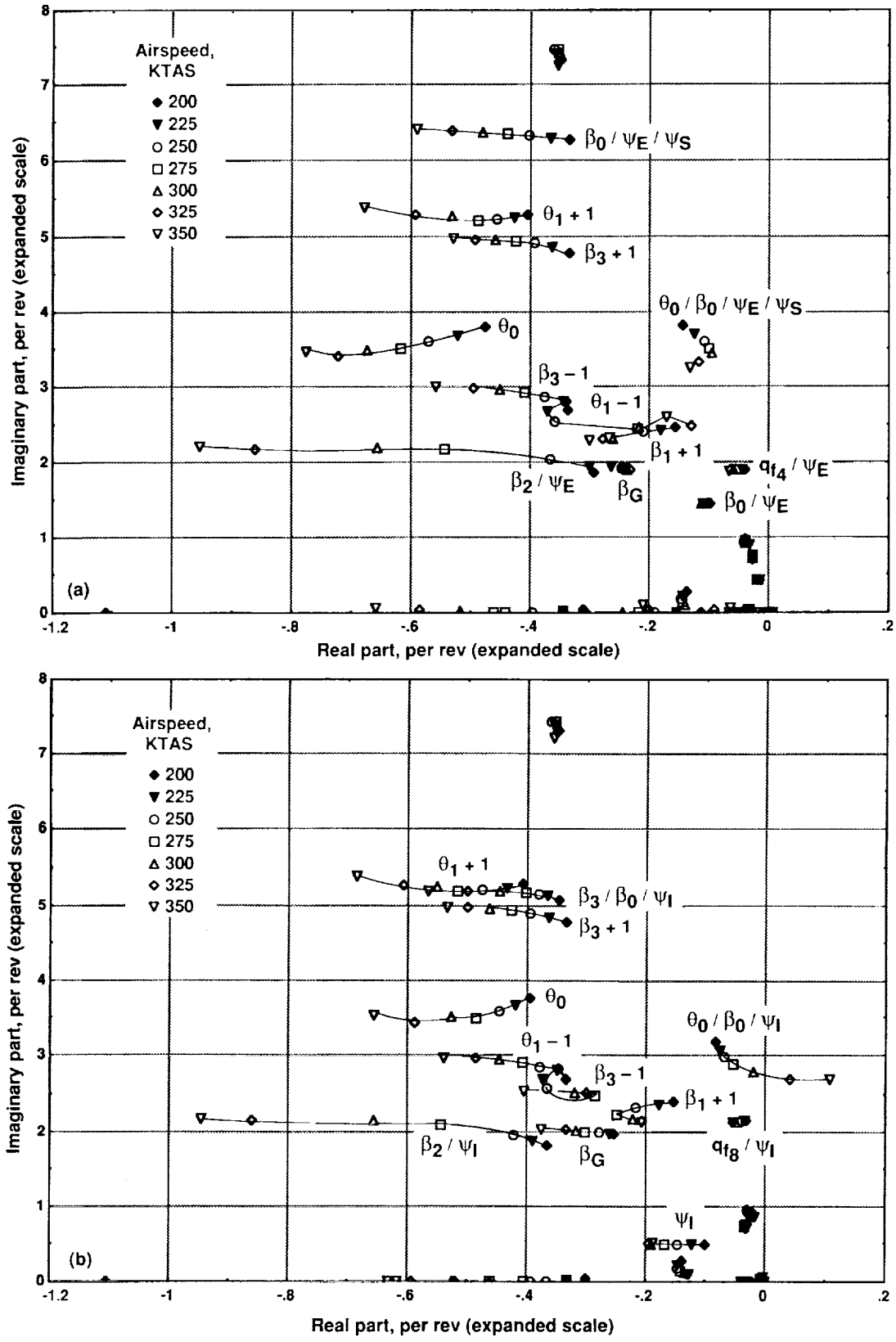

Figure 13. Eigenvalues for corrected model with 1° sweep, standard tips, and full control-system stiffness matrices; 200-350 KTAS speed variation at 80% rotor speed. (a) Symmetric modes. (b) Antisymmetric modes.

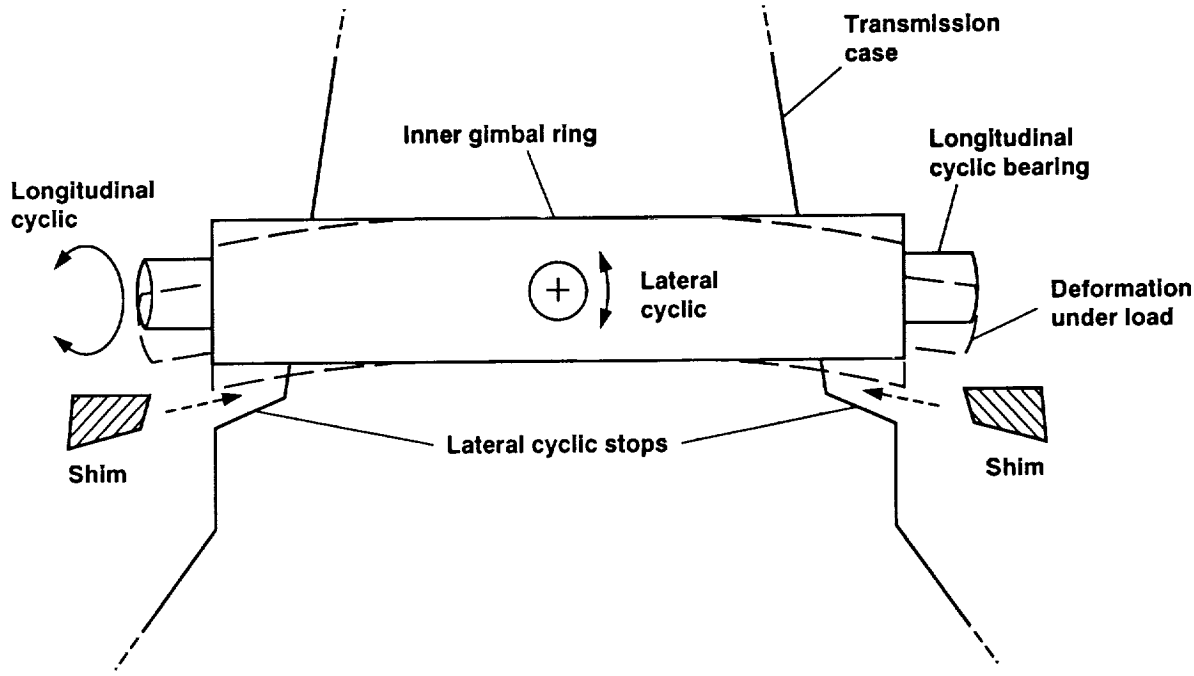

Figure 14. Schematic of inner gimbal ring and shim installation (not to scale; deformations are exaggerated).

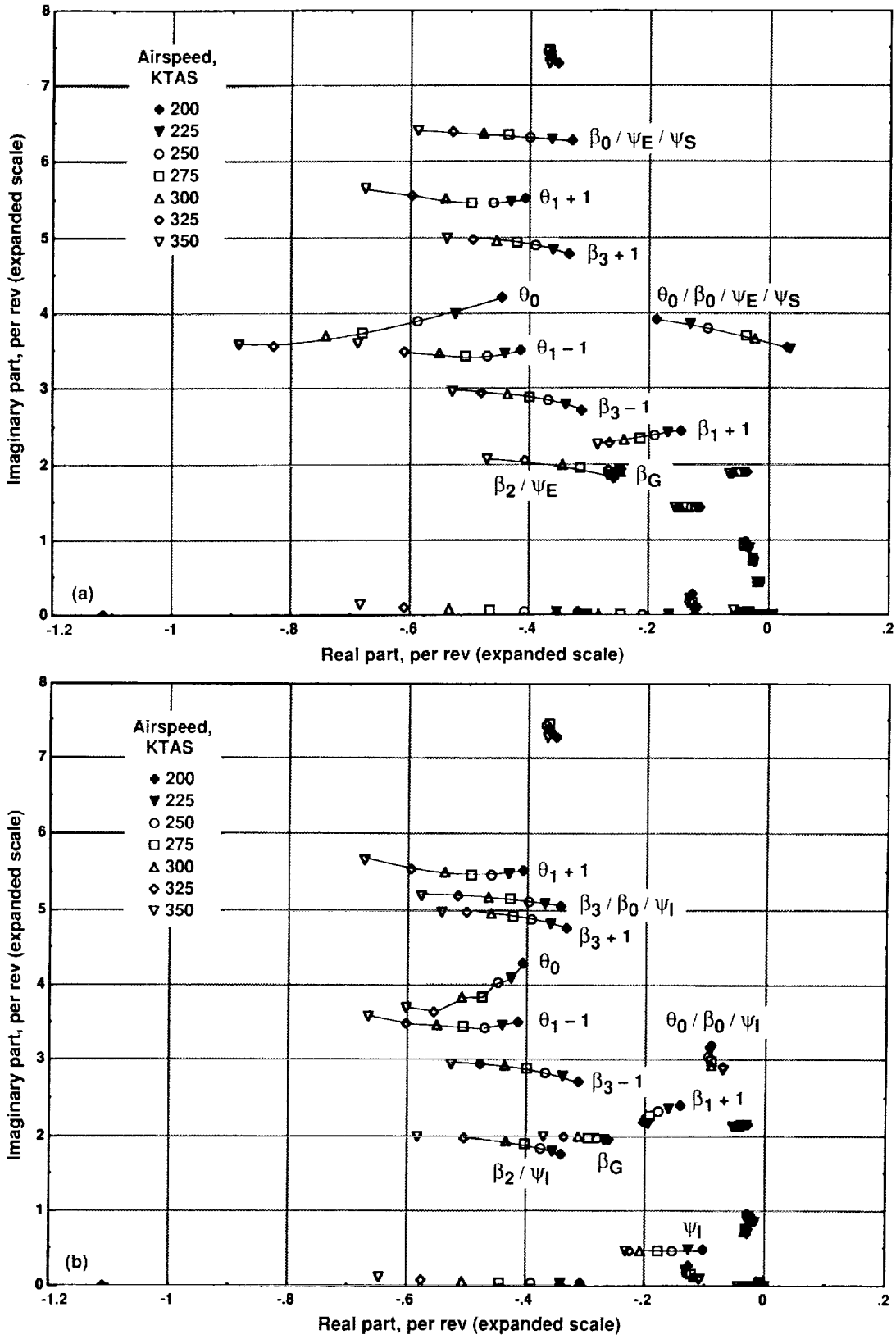

Figure 15. Eigenvalues for corrected model with 1° sweep, standard tips, and stiffness matrices for shimmed control system; 200-350 KTAS speed variation at 80% rotor speed. (a) Symmetric modes. (b) Antisymmetric modes.